

EXPERIMENTAL ANALYSIS ON BOUNDARY LAYER GROWTH USING VARYING CONFIGURATION OF ROUGHNESS BLOCKS AND SPIRES IN WIND TUNNEL

Thesis submitted to the
National Institute of Technology, Rourkela
in partial fulfillment of the requirements
for the dual degree of

Bachelor and Master of Technology
in
Civil Engineering
(*PG Specialization: Water Resources Engineering*)

by

Rishabh Prakash
(*Roll Number: 711CE4099*)

Under the supervision
and guidance of

Prof. Awadhesh Kumar



May 30, 2016

Department of Civil Engineering
National Institute of Technology, Rourkela
Odisha - 769008, India



**Department of Civil Engineering
National Institute of Technology, Rourkela
Odisha, 769008, India**

May 30, 2016

CERTIFICATE OF EXAMINATION

Roll Number: **711ce4099**

Name: **Rishabh Prakash**

Title of Dissertation: **Experimental analysis on boundary layer growth using varying configuration of roughness blocks and spires in wind tunnel**

We the below signed, after checking the dissertation mentioned above and the official record book (s) of the student, hereby state our approval of the dissertation submitted in partial fulfilment of the requirements of the degree of Doctor of Philosophy in Computer Science and Engineering at National Institute of Technology Rourkela. We are satisfied with the volume, quality, correctness, and originality of the work.

External Examiner

Prof. Awadhesh Kumar
Department of Civil Engineering,
National Institute of Technology, Rourkela



Department of Civil Engineering
National Institute of Technology, Rourkela
Odisha, 769008, India

May 30, 2016

SUPERVISOR'S CERTIFICATE

This is to certify that this thesis entitled “**Experimental analysis on boundary layer growth using varying configuration of roughness blocks and spires in wind tunnel**”, put together by **Mr. Rishabh Prakash**, bearing the roll number **711CE4099**, a B. Tech and M. Tech Dual Degree scholar in the Civil Engineering Department, National Institute of Technology, Rourkela, in partial fulfilment for the award of the dual degree of **Bachelor of Technology in Civil Engineering** and **Master of Technology in Water Resources Engineering**, is a bona fide record of a genuine research work completed by him under my guidance and supervision. This thesis has satisfied all the necessities according to the regulations of the Institute and has, in my opinion, come to the standard required for submission. The results included in this thesis have not been uploaded/submitted to any other institute or university for any academic award, degree or diploma.

Date:

Place:

Prof. Awadhesh Kumar

Department of Civil Engineering,
National Institute of Technology, Rourkela

Dedicated to all the budding
Water Resources Engineers
and
my beloved friends

DECLARATION OF ORIGINALITY

I, **Rishabh Prakash**, Roll Number **711CE4099**, at this moment declare that this thesis entitled **“Experimental analysis on boundary layer growth using varying configuration of roughness blocks and spires in wind tunnel”** represents my original work carried out as a dual degree student of National Institute of Technology, Rourkela. And, the best of my knowledge, it contains no material previously published or written by another person, nor any material presented for the award of any other degree or diploma of National Institute of Technology, Rourkela or any other institution. Any contribution made to this research by others, with whom I have worked at National Institute of Technology, Rourkela or elsewhere, is explicitly acknowledged in the thesis. Works of other authors cited in this thesis have been duly recognized under the section "Bibliography". I have also submitted my original research records to the scrutiny committee for evaluation of my thesis.

I am acutely aware that in the case of any non-compliance detected in future, the Senate of National Institute of Technology, Rourkela may withdraw the degree awarded to me by the present thesis.

May 30, 2016
NIT Rourkela

Rishabh Prakash
Roll Number: 711CE4099

ACKNOWLEDGEMENTS

My most recent five years venture at **National Institute of Technology, Rourkela** has added significant and valuable experiences to my life. I have utmost regard and adoration for this institute and I will always remember the individuals who have made this environment so exceptional and extraordinary. Now it is time to proceed onward to my future. Before I go any further, I like to express my sincere gratitude to those who have assisted me along the way.

First and foremost, praise and heartfelt thanks go to the Almighty for the blessing that has been showered upon me in all my endeavours.

I would like to express profound gratitude to my project supervisor, **Prof A. Kumar** for furnishing me with a stage to chip away at an incredibly energizing and testing field of **Experimental analysis on boundary layer growth using varying configuration of roughness blocks and spires in wind tunnel**. His untiring exertion, commitment and way of supervision is highly brain stimulating and extracts the best from a student. He has regularly given me the opportunity to envision, execute and analyse, but has coincidentally guided me sharply to keep on track throughout the project work. It has helped me a lot for self-development for which I am obliged the most.

It gives me immense pleasure to acknowledge my batch mates, **Prayas** and **Prasang**, and seniors of Department of Civil Engineering for their help, constant encouragement, motivation and suggestions for my project work.

Most importantly, this would not have been possible without the affection and support of my Family. They have been a constant source of love, concern, support and strength all these years. I would like to express my heart-felt appreciation to them.

May 25, 2016
NIT Rourkela

Rishabh Prakash
Roll Number: 711CE4099

ABSTRACT

Flowing behaviour of real fluid is very complex to understand. When real fluid flows over a solid body or a solid plate, the fluid particles adhere to the boundary of the stationary surface and the phenomenon of no slip condition occurs. This results that the velocity of fluid near to the boundary will be same as that of boundary. If the boundary is stationary, the velocity of fluid at the boundary will be zero. The velocity of fluid increases from zero velocity on the stationary boundary to the free stream velocity of the fluid in the direction normal to the boundary. Boundary layer is defined by its parameters as boundary layer thickness, momentum and displacement thickness. In boundary layer region viscous effect is prominent; drag force and shear force act within this layer on the body. Study of boundary layer is important for design of stream line bodies such as air foils. Most wind tunnels, typically designed for the study of aeronautics with smooth laminar flow, lack the turbulence intensity and sufficient boundary layer depths. The present work shows how thick boundary layers can be produced in a wind tunnel with a view to simulate atmospheric flows. The wind loading on structures depends on the velocity and turbulence parameters of the approaching flow. Therefore, in order to obtain similitude between the model loading in the wind tunnel and the real structure, different types of thickening devices are used which are 2.5 cm cube blocks as a floor roughness and 45cm height spires of different configurations in test section. Analysed the effect of different patterns of spires and floor roughness blocks on boundary layer parameter in test section using velocity profiles at variable free stream velocity, were measured at five sections in test section. And roughness parameter was measured for all configurations of spires and blocks using log-law of velocity profiles.

This paper summarizes the recent investigations involving the computations of effects of roughness thickness, mainstream velocity and distance from roughness plate on turbulent boundary layer along with the correlations.

Keywords: Fluid; Wind tunnel; spires; boundary layer; turbulence; roughness.

TABLE OF CONTENTS

CERTIFICATE OF EXAMINATION.....	ii
SUPERVISOR’S CERTIFICATE.....	iii
DECLARATION OF ORIGINALITY.....	v
ACKNOWLEDGEMENTS	vi
ABSTRACT.....	vii
TABLE OF CONTENTS	viii
LIST OF FIGURES	xi
LIST OF TABLES	xiv
ABBREVIATIONS	xv
CHAPTER 1 : INTRODUCTION.....	1
1.1 BASIC PROPERTIES OF WIND TUNNEL	1
1.2 BOUNDARY LAYER.....	1
1.3 ATMOSPHERE BOUNDARY LAYER (ABL).....	2
1.4 BOUNDARY LAYER (BL) THICKNESS	4
1.5 SIMULATION OF ABL IN WIND TUNNEL (WT)	5
1.6 DIFFERENT PARAMETER OF BOUNDARY LAYER.....	6
1.6.1 Displacement thickness(δ^*):	6
1.6.2 Momentum thickness (θ):.....	6
1.7 WIND TUNNEL AND ITS CLASSIFICATION	7
1.7.1 First Type classification: Based on structure of Wind Tunnel	7
1.7.2 Second type classification: Based on speed in WT	7
CHAPTER 2 : OBJECTIVES	8
CHAPTER 3 : LITERATURE REVIEW	9
3.1 GENERAL	9
CHAPTER 4 : EXPERIMENTAL SETUP AND METHODOLOGY.....	14

4.1	GENERAL	14
4.2	WIND TUNNEL USED FOR EXPERIMENT:	14
4.2.1	DRIVING UNIT:.....	14
4.3	EQUIPMENTS:.....	15
4.3.1	TELESCOPIC PROBE VELOCITY METER:.....	16
4.3.2	DIGITAL VELOCIMETER MODEL A00TSI:	16
4.3.3	TACHOMETER:.....	17
4.3.4	TROLLEY:.....	17
4.3.5	ROUGHNESS SQUARE BLOCKS:.....	18
4.3.6	SPIRES ARRANGEMENT:	19
4.3.7	COMBINATION OF SPIRES WITH ROUGHNESS BLOCKS:	20
4.4	SET-UP	20
4.5	METHODOLOGY	21
CHAPTER 5 : RESULTS AND DISCUSSION		22
5.1	OVERVIEW.....	22
5.2	VELOCITY PROFILES FOR DIFFERENT ARRANGEMENTS OF BLOCKS .	22
5.3	VELOCITY PROFILES FOR DIFFERENT ARRANGEMENTS OF SPIRES AND BLOCKS AT CONSTANT FREE STREAM VELOCITY:	25
5.4	VARIATIONS IN BOUNDARY LAYER FOR ALL ARRANGEMENT AT CONSTANT VELOCITY	27
5.5	VARIATION IN BOUNDARY LAYER FOR SAME ARRANGEMENT AT VARYING FREE STREAM VELOCITIES:	29
5.6	ESTIMATION OF ROUGHNESS LENGTH FOR DIFFERENT ARRANGEMENTS	31
5.7	CALCULATIONS OF PARAMETERS OF BOUNDARY LAYER:	34
5.7.1	Calculations method of boundary layer parameters:	34
5.8	CORRELATION OF VARIABLES:	41
5.8.1	Exponent's determination for BL thickness (δ):.....	42

5.8.2	Exponent's determination for displacement thickness:	44
5.8.3	Correlation exponent's determination for Momentum thickness θ :.....	46
5.9	COMPARISON GRAPHS FOR BOUNDARY LAYER PARAMETERS:	51
5.10	DISCUSSION	52
CHAPTER 6 : CONCLUSIONS		54
6.1	CONCLUSIONS	54
6.2	SCOPE FOR FUTURE WORK	55
REFERENCES.....		56

LIST OF FIGURES

Figure 1.1: Variations in ABL for a day	3
Figure 1.2: Different parts of ABL	5
Figure 1.3: δ^* Displacement thickness.....	6
Figure 3.1: Irwin arrangements in Wind Tunnel	12
Figure 3.2: Arrangement of array of cylindrical rods and on rectangular bar	13
Figure 4.1: Wind tunnel at NIT Rourkela	15
Figure 4.2: Driving unit of Wind Tunnel	15
Figure 4.3: Digital velocity meter	16
Figure 4.4: Digital velocity meter	16
Figure 4.5: Tachometer	17
Figure 4.6: Trolley Arrangement	17
Figure 4.7: Square pattern of 1 inch cube blocks	18
Figure 4.8: Diamond pattern 1 inch cube blocks	18
Figure 4.9: Spires with 18cm and 6 spacing respectively	19
Figure 4.10: Spires with 18cm spacing	19
Figure 4.11: Spires with diamond and square arrangement of cube blocks	20
Figure 4.12: Test section of NITRKL Wind Tunnel.....	21
Figure 5.1: Velocity profiles for different arrangements of blocks at $V=11.19\text{m/s}$	23
Figure 5.2: velocity profiles for different arrangements of blocks at $V=9.32\text{m/s}$	24
Figure 5.3: velocity profiles for different arrangements of blocks at $V=7.67\text{m/s}$	25
Figure 5.4: velocity profiles at $V=11.19\text{m/s}$	26
Figure 5.5: velocity profiles at $V=9.32\text{m/s}$	26
Figure 5.6: velocity profiles at $V=7.67\text{m/s}$	27

Figure 5.7: Boundary layer thickness at $V=11.31\text{m/s}$	27
Figure 5.8: Boundary layer thickness at $V=9.32\text{m/s}$	28
Figure 5.9: Boundary layer thickness at $V=7.67\text{m/s}$	28
Figure 5.10: BL thickness for empty Wind Tunnel	29
Figure 5.11: BL thickness for square pattern of blocks	29
Figure 5.12: BL thickness for diamond pattern of blocks	29
Figure 5.13: Boundary layer variation for spire with diamond configuration of blocks	30
Figure 5.14: Boundary layer variation for spires with square configuration of blocks	30
Figure 5.15: Boundary layer variation for spires with 6cm c/c spacing	30
Figure 5.16: Boundary layer variation for spires with 12 cm c/c spacing	31
Figure 5.17: Boundary layer variation for spires having c/c spacing 18cm.....	31
Figure 5.18: Estimation of roughness length for square pattern of blocks.....	32
Figure 5.19: Roughness length estimation in WT for diamond pattern of blocks.....	32
Figure 5.20: Roughness length estimation for spires with square pattern of blocks	33
Figure 5.21: Roughness length estimation for spires with diamond pattern of blocks	33
Figure 5.22: Graph for square pattern blocks at $V=7.67\text{ m}$, $x=20\text{cm}$ from roughness plate...	34
Figure 5.23: Graph for diamond pattern of blocks at $V=7.67\text{ m}$, $x=20\text{cm}$ from roughness plate	35
Figure 5.24: Graph for diamond pattern of blocks at $V=9.31\text{m/s}$, $x=20\text{cm}$ from roughness plate	35
Figure 5.25: Graph for diamond pattern of blocks at $V=9.32\text{m/s}$, $x=60\text{ cm}$ from roughness plate	36
Figure 5.26: Graph for square pattern of blocks at $V=11.19\text{m/s}$, $x=20\text{cm}$ from roughness plate:	36
Figure 5.27: Graph for spires with diamond pattern of blocks at $V=11.19\text{m/s}$, $x=20\text{cm}$ from roughness plate	37

Figure 5.28: Graph for spire with square pattern of blocks at $V=11.19\text{m/s}$, $x=20\text{cm}$ from roughness plate	37
Figure 5.29: Graph for spire with diamond pattern of blocks at $V=9.31\text{m/s}$, $x=20\text{cm}$	38
Figure 5.30: Graph for spire with square pattern of blocks at $V=9.31\text{m/s}$, $x=20\text{cm}$ from trailing edge	38
Figure 5.31: Graph for spire with diamond pattern of blocks at $V=7.67\text{m/s}$, $x=20\text{cm}$ from roughness plate	39
Figure 5.32: Graph for spires with square pattern of blocks at $V=7.67\text{m/s}$, $x=20\text{cm}$ from roughness plate	39
Figure 5.33: Roughness exponent determination for BL thickness	42
Figure 5.34: Velocity exponent determination for BL thickness	42
Figure 5.35: Distance exponent determination for BL thickness	43
Figure 5.36: Correlation plot for system variable with BL thickness	43
Figure 5.37: Roughness exponent for δ^*	44
Figure 5.38: Estimation of Velocity exponent for δ^*	44
Figure 5.39: Estimation of exponent of X for δ^*	45
Figure 5.40: Correlation plot for system variable with δ^*	45
Figure 5.41: Estimation of roughness exponent for θ	46
Figure 5.42: Estimation of velocity exponent for θ	46
Figure 5.43: Estimation the exponent of X for θ	47
Figure 5.44: Correlation plot for system variables with θ	47
Figure 5.45: Comparison between experimental and predicted (δ)	51
Figure 5.46: Comparison between experimental (δ^*) and predicted (δ^*)	51
Figure 5.47: Comparison between experimental (θ) and predicted (θ)	52

LIST OF TABLES

Table 1.1: Classification based on speed.....	7
Table 4.1: Wind tunnel specifications.....	14
Table 5.1: Roughness thickness for all configuration.....	33
Table 5.2: Calculated values of BL parameters with system variables.....	40
Table 5.3: Values of exponents and constant for boundary layer parameters obtained from correlation.....	48
Table 5.4: Comparison between experimental and predicted value (δ) obtained from correlation	48
Table 5.5: Comparison between experimental and predicted value of (δ^*) obtained from correlation.....	49
Table 5.6: Comparison between experimental and predicted value of (θ) obtained from correlation.....	50

ABBREVIATIONS

ABL	Atmospheric Boundary Layer
WT	Wind Tunnel
BL	Boundary Layer
τ	Surface Shear Stress
μ	Dynamic Viscosity
dv/dy	Velocity Gradient
V	Free Stream Velocity
M	Mach No
Re	Reynolds Number
y	Vertical Height from Wind Tunnel surface
X	Distance from the Trailing edge
Z ₀	Roughness length
δ	Boundary Layer Thickness
δ^*	Displacement Thickness
θ	Momentum Thickness
R ²	Regression Co-efficient
B	Constant Correlation Coefficient
ZPG	Zero Pressure Gradient

CHAPTER 1: INTRODUCTION

1.1 BASIC PROPERTIES OF WIND TUNNEL

Wind and turbulence is experienced in regular life. We can define wind in simple words that moving form of air. We can't see wind but we can see its effects very easily on earth everywhere. The momentary wind mainly involved 3 parts, the mean wind speed, a periodic or occasional velocity of wave and irregular fluctuating speeds. Wind has its own advantages and disadvantages as strong wind can be destructive for human life and buildings but in dispersion for air pollution and in production of wind energy it is benefited for human. In 2005 Katrina hurricane damaged 75 billion USD property in US. Wind can classified by its characteristics location and strength. Most common wind type that affects severely to human life are tornadoes and hurricanes. A tornadoes is rotating column system of air which is in funnel shape near the ground whereas hurricanes are tropical region cyclones. Wind flow near the ground on earth is highly turbulent in nature due to the roughness characteristic of ground. Turbulent is basic property of wind but it is very complex phenomenon to understand for human. One time the famous fluid mechanic, Theodore von Karman, is stated:

‘There are two great unexplained mysteries in our universe. One is the nature of a unified generalized theory to explain both gravity and electromagnetism. The other is an understanding of the nature of turbulence. After I die, I expect that God will clarify the general field theory to me. I don't have such hope for turbulence’

Turbulence can characterized by the features (1) Irregularity (2) Diffusivity (3) Rotationally (4) Dissipation.

1.2 BOUNDARY LAYER

The concept of the boundary layer was developed by Prandtl in 1904. When a fluid flows over an object at high Reynolds number than layer of fluid in the immediate vicinity of solid surface where the effects of viscosity are significant is known as boundary layer and at surface of boundary fluid has zero velocity which is no-slip condition but away from the solid surface velocity increase or velocity gradient exists. There are mainly two types of boundary layer flow first is laminar and other is turbulent flow. Laminar flow is straight line flow and in laminar flow skin drag force is very small so it smooth type flow but in turbulent flow skin friction is

prominent and it's very irregular and random flow due to eddies formations. There are more mixing finite size eddies than laminar in turbulent flow.

1.3 ATMOSPHERE BOUNDARY LAYER (ABL)

Atmosphere of earth is divided into four parts and its height more than 100 km but ABL is within lowest part of atmosphere which means it is in troposphere. Troposphere height is less than 10 km from the earth surface and it is most important layer for human because weather system and other all weather related activity occur mostly in this layer like hurricane tornado and all other activity. Why ABL is so important? Main reason is that within ABL depth wind characteristic that is laminar or turbulent and other properties will change due to the effect of surface characteristic of earth, temperature and shear force is vary within region of ABL thus wind load become more effective within ABL region. So ABL become more important for design purpose of man-made structure. Most Wind Tunnel is not designed for turbulent flow, turbulent intensity and having insufficient BL depth. Wind tunnel turbulent intensity is not more than 5% whereas expect plain area in earth ABL turbulent intensity is always more than 5%, so model test in WT for this regions will not give correct and suitable result. In long test section supersonic and sub sonic WT we can generate turbulent flow but thickness of boundary layer is very less. In NITRKL subsonic type 8m long test section WT is having maximum BL thickness is 12cm to 14cm without using any passive device and wind speed is approx. 7m/s. Within ABL surface of earth and all man-made structure feels shear stress due to velocity gradient and enhance the effect of wind load on structures. Planetary boundary layer (PBL) is second name of ABL so both are same.

ABL flow having main characteristics is turbulent and it have temporal and spatial variable.

Reynolds derived expression for flow field in ABL and this expression divide flow field into two components first is mean and second is fluctuating component.

$$u(\vec{r}, t) = u(\vec{r}, t) \vec{i} + v(\vec{r}, t) \vec{j} + w(\vec{r}, t) \vec{k}$$

$$u(\vec{r}, t) \vec{i} = \bar{u}(\vec{r}) + u'(\vec{r}, t) \vec{i}$$

Mean velocity is $\bar{u}(\vec{r})$ is defined as

$$\bar{u}(\vec{r}) = \lim_{T \rightarrow \infty} \frac{1}{T} \int_0^T \bar{u}(\vec{r}, t) dt$$

ABL, it has three types first neutral (NBL) second, convective (CBL) and last is stable boundary layer. Interaction of earth surface and air occur mainly by two methods, first, mechanical and second, thermal. In mechanical interaction friction is generated by contact with wind and earth surface and turbulent generate through this phenomenon. Whereas in second type interaction, thermal by temperature difference between lower atmosphere and earth surface. NBL, it is transition between stable and unstable condition and in NBL temperature gradient is very less so strong turbulent will generate near the surface due to strong shear force. NBL is time limited phenomenon and the atmosphere of neutral is occurs either morning time or evening time in a day. Mainly when small temp. Gradient is exist between earth surface and above air of the surface of earth. CBL is also called unstable boundary layer. In CBL generally earth surface is hotter than air above the earth surface. So here temperature gradient is not very small, like NBL. In CBL turbulent kinetic energy (TKE) and momentum transfer between layers is enhanced by temperature difference.

Stull (1988) developed expression for wind profile over flat region.

$$U(z) = \frac{u_*}{\kappa} \left[\ln \left(\frac{z}{z_0} \right) - \psi_m \left(\frac{z}{L} \right) \right]$$

u_* Friction velocity κ , von Karman constant (≈ 0.4) z_0 aerodynamic roughness length and ψ_m is function of $\frac{z}{L}$, L is Obukhov length, $L = \frac{-\bar{\theta} u_*^3}{\kappa g (\overline{\omega' \theta'})_s}$, $\bar{\theta}$ is temperature, g is gravitational acceleration, and $(\overline{\omega' \theta'})_s$ heat flux.

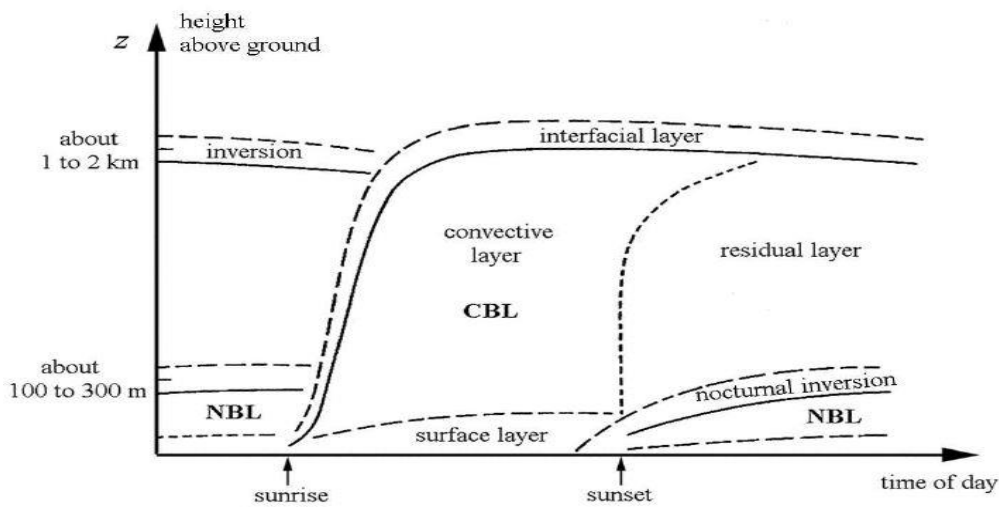


Figure 1.1: Variations in ABL for a day

1.4 BOUNDARY LAYER (BL) THICKNESS

Simply boundary layer thickness define is, fluid flow over the solid surface if surface is not moving then on solid surface fluid particle will stick and velocity become zero and in normal to solid surface velocity increases. From solid surface to that point where velocity become $0.99U$ in normal direction is called thickness of boundary layer. Thickness of ABL is depend of many factor as roughness condition, temperature and wind speed. ABL is mainly turbulent flow and thickness vary but on land thickness is 1km to 2km and on ocean thickness is approx. 0.5km. Within the range shear force act due velocity gradient.

ABL divided into two parts upper part and lower part, upper part known as outer layer or Ekman layer and lower part is inner layer it is shown in fig no.1 (d). Again inner layer divided in two parts which are known as interfacial sub layer and inertial sub layer but here main difference between inner layer and outer layer is that inner layer is affected by characteristics of earth surface but outer surface is not. In inner interfacial sub layer depth is directly depend on roughness of land surface means in open plain where the roughness is very less so there we can assume zero depth for interfacial sub layer. IS 875 (part 3) describe, the terrain are divided in mainly four part and these are

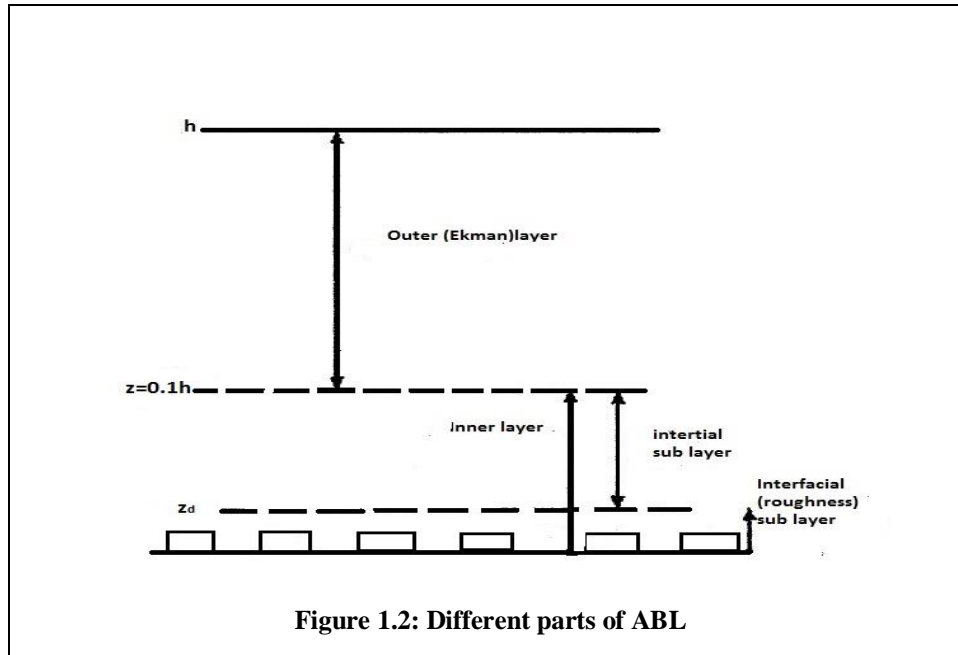
Category 1- mainly it consist open terrain or obstacle height should not more than 1.5m example coastal area of sea or treeless ground.

Category 2- obstruction height more than 1.5 but less than 10 m example rural area.

Category 3- obstruction is more than 10 m and not dense packed area just scattered obstacles like sub urban area.

Category 4- dense paced area which consists more obstacles which having height more 10 like urban area of India.

All four terrain having different height and properties of outer layer and inner layer mainly inner layer which shown in following figure:



1.5 SIMULATION OF ABL IN WIND TUNNEL (WT)

In wind tunnel as we know, cannot generate sufficient height of boundary layer and turbulence, commonly Wind Tunnel is designed for smooth type laminar flow which have less than 4% turbulence. Many researcher use passive devices like vortex generator (spires), fence, roughness and other devices in WT to enhance turbulence and depth of boundary layer, this is known as augmentation devices.

First time in 1960's Counihan used elliptical shape generator in WT to enhance the turbulence and depth of BL then many other research developed more other passive devices, and some use jet on WT floor. In simulation of ABL develop the BL in WT which having same turbulence characteristics as ABL and for simulation generally use power-law equation

$$\frac{u}{U} = \left(\frac{z}{\delta}\right)^{\alpha}$$

u is mean velocity, δ is depth of boundary layer, z is height from the surface α defined by roughness of terrain as 0.1 for open sea terrain and 0.35 for urban area (>10m height) different range of α according to terrain can achieved in WT by using of different passive devices.

In this experimental study 2.5cm cube roughness blocks of different arrangement and triangular spires, size is 45 cm are used as roughness elements in Wind Tunnel. This experimental study 1inch blocks in different patterns used as floor roughness, and combination of spires with

roughness blocks to study the effect on boundary layer at wind speeds 6.7m/s, 9m/s and 10.3m/s in Wind Tunnel. Due to momentum loss depth of boundary layer increased in WT. By using floor roughness BL depth is increased by about 80% to 100% of empty WT BL (boundary layer).

1.6 DIFFERENT PARAMETER OF BOUNDARY LAYER

Important parameters to analyze the shape and size of boundary layer over the solid surface for real fluid flow are mainly boundary layer thickness, momentum thickness and displacement thickness.

1.6.1 Displacement thickness(δ^*):

Displacement thickness is define as the distance by which the surface boundary should displace in parallel direction to compensate for the reduction in flow rate due to formation of boundary layer over the solid surface for real fluid.

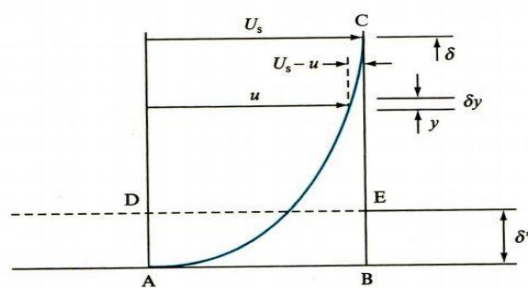


Figure 1.3: δ^* Displacement thickness

Mathematical express for displacement thickness,

$$\delta^* = \int_0^{\delta} \left(1 - \frac{u}{U}\right) dy$$

1.6.2 Momentum thickness (θ):

Momentum thickness defines the distance by which surface boundary should displace in parallel direction to itself to compensate for loss in momentum because of boundary layer formation over the solid surface for real fluid.

Mathematical express for momentum thickness θ ,

$$\theta = \int_0^{\delta} \frac{u}{U} \left(1 - \frac{u}{U}\right) dy$$

1.7 WIND TUNNEL AND ITS CLASSIFICATION

Wind tunnel (WT) is man- made tunnel it use for generating the artificial wind at different speed.it is useful to study the flow and its pattern at different speed, useful for to know wind load on different objects and it is main use to understand the aerodynamics properties like streamline flow, drag, lift and pitching moment.

1.7.1 First Type classification: Based on structure of Wind Tunnel

Close circuit WT:

This is closed circuit structure means air circulate in this WT and no need of fresh air from surrounding area. This type WT size is bigger than open circuit WT.

Open circuit WT:

It open circuit type structure in this type WT it takes directly air form surrounding environment and this structure is not so big as close circuit

1.7.2 Second type classification: Based on speed in WT

By Mach No we classified WT in different group which directly based on speed of fluid in WT.

$$\text{Mach No. (M)} = \frac{V}{c} \quad (c = \text{velocity of sound})$$

Table 1.1: Classification based on speed

Mach No.(M)	Type of flow in WT
M<1	Subsonic
1<M<3	Supersonic
3<M<5	High supersonic
M<5	Hypersonic

CHAPTER 2: OBJECTIVES

Present work main objective to study the effects of different configurations of spires and roughness blocks on boundary layer growth and different parameter of boundary layer in test section of Wind Tunnel.

Objectives of present work are categorized as-

1. To measure the effect of 2.5cm cube of roughness blocks and 45cm height spires of different configurations, at varying free stream velocity on velocity profiles and boundary layer thickness in test section of Wind Tunnel by experimentally.
2. To measure the roughness parameter in test section for different patterns of spires and roughness blocks using experimental analysis.
3. To determine the momentum thickness, displacement thickness using velocity profile at different sections for varying configurations of blocks and spires in test sections.
4. To establish Correlation for boundary layer parameters in function of independent variables, which are roughness length, distance from trailing edge and free stream velocity in test section.

CHAPTER 3: LITERATURE REVIEW

3.1 GENERAL

In these literatures consist the work of many engineer and scientist of all world who worked on simulation of ABL in WT by different methods and developed the relations for passive devices to boundary layer and also its different parameters. As we in wind tunnel BL thickness is very low and turbulence is low so all scientist used active devices as well as passive of different sizes and also established the relations for boundary layer growth.

Stevenson (1880) first time gave parabolic law for velocity profile which was valid for more than 10m height from the surface. For some limit it gives correct representation of velocity profile.

$$\frac{V}{v} = \sqrt{\frac{z+22}{z_{ref}+22}}$$

z_{ref} And z are in meters

Hellman (1916) established an empirical for velocity profile which corrected from of Stevenson's parabolic equation, Hellman proposed power law which depends upon not only height from ground but also on characteristics of terrain.

$$\frac{V}{v} = \left(\frac{z}{z_{ref}} \right)^\alpha \quad \alpha \text{ is defined by characteristics of ground}$$

This power-law is also not valid for up to 10 height from earth surface but it is more accurate than Stevenson (1880)'s law for more than 10m height.

Sutton (1949) derived an equation which can measure mean velocity profile for lower than 10m. velocity profile through Sutton equation's not follow parabolic path but there is logarithmic relation.

$$\bar{u} = \frac{1}{k} u_* \ln \left(\frac{z-z_d}{z_0} \right) ; k = 0.4$$

k is defined as Von Karman constant this is experimental value and depend on experiments in WT and also in atmosphere. z_d Is defined as zero plane displacement which is the lowest part of ABL. z_0 , defined as aerodynamic roughness, is a distance from surface where velocity is zero due to the effect of surface roughness. u_* Friction velocity.

Urban	$2\text{m} < z_0 < 3\text{m}$
Suburban	$0.2\text{m} < z_0 < 1.2\text{m}$
Rural	$0.001\text{m} < z_0 < 0.2\text{m}$
Smooth	$0.0001\text{m} < z_0 < 0.006\text{m}$

The fiction velocity,

$$u_* = \sqrt{\frac{\tau_w}{\rho}}$$

$$\tau_w \text{ Is wall shear stress, } \tau_w = \mu \left(\frac{d\bar{u}}{dy} \right)_{y=0}$$

G.I. Taylor (1915-1938) experimentally analysis the turbulence in WT and propound the theory that velocities can be divided into two part, spatially and second temporally.

$$Lu_x = \bar{u} \cdot \int_0^\infty R(\tau) d\tau$$

This equation is Tylor's hypothesis and $R(\tau)$ is autocorrelation

Townsend (1957) is designed first time triangular spires and studied the effect on BL in WT and he found that in inner region momentum loss is excess but in outer region is lack of momentum loss. It produces large eddies and at the surface large turbulence generated. It generated model flow in outer region and inner in the region of BL.

Kline et al. (1967) studied the turbulent structure in WT which is mainly caused by turbulence production rate and in normally developed BL the turbulent structure is formed near the wall due to eddies near the wall and high speed flow in direction of wall, this is also known as wall-layer streak and due to this turbulence kinetic energy transferred to outer region of BL in WT.

Counihan (1969) designed an elliptical generator that is quarter elliptical and minor axis is half of the major axis and he carried out experiment with two types of elliptical wedges whose angles are 5° and 6° . In elliptical type generator turbulence is high and constant unlike to triangular generator. Counihan used elliptical generator for experimental analysis which having major axis 100mm and minor axis is half of major that is 50mm and between them was 70mm. Again he did some modification for urban type simulation of ABL in WT. for modification he used Lego brick for roughness which sizes were 9.5 mm square and 5.9mm and arranged it on baseboard and placed on floor of WT. He also studied the wake formation behind the generator and differentiated the wake behind triangular generator and elliptical generator.

Hunt and Fernholz (1975) propounded 10 simple methods for simulation of stable, neutral and unstable ABL in different type Wind Tunnel for this they used the different combination of spires, wedge and different roughness element on floor of Wind Tunnel, it is a simple way to increase the boundary layer depth in Wind Tunnel. They carried out their experiments in different 28 Wind Tunnel and classified their simulation methods into three parts according to Hunt and Fernholz.

1. Only change the floor roughness in wind tunnel by using different pattern roughness blocks and analyzed the effect on BL.
2. In this method both outer and inner zone in boundary layer has been changed by using active devices which is generally multiple jets are placed at entrance of working section and on floor of Wind Tunnel
3. Mainly in this method generally use spires and other same vortex generator which can alter irrotational flow in Wind Tunnel. In this method turbulent wake form behind the spires and because of momentum loss boundary layer is increased.

N.J. Cook (1978) simulate adiabatic ABL by roughness blocks, barrier and mixing device in Wind Tunnel. Here roughness gave best simulation result over roughness length and enhanced the BL by barrier. If wind speed is more than 10m/s known as adiabatic ABL. in roughness

block he used 25mm to 100mm size cube and mixing device generally he used elliptical wedge that is vortex generator and plain wall less height than elliptical wedge as barrier in Wind Tunnel and he found momentum deficit is mainly by strong wake generation behind the elliptical wedge.

Irwin (1980) introduced formula for design of triangular spires for simulation of ABL in Wind Tunnel. In fig.no.3.1 shows the arrangement in Wind Tunnel for simulation. He established the relation between height of triangular spires and BL thickness.

$h = 1.39\delta / (1 + \alpha/2)$, h , height of spires and α , exponent for power-law

$$\frac{U}{U_\delta} = \left(\frac{z}{\delta}\right)^\alpha, \quad \text{power-law}$$

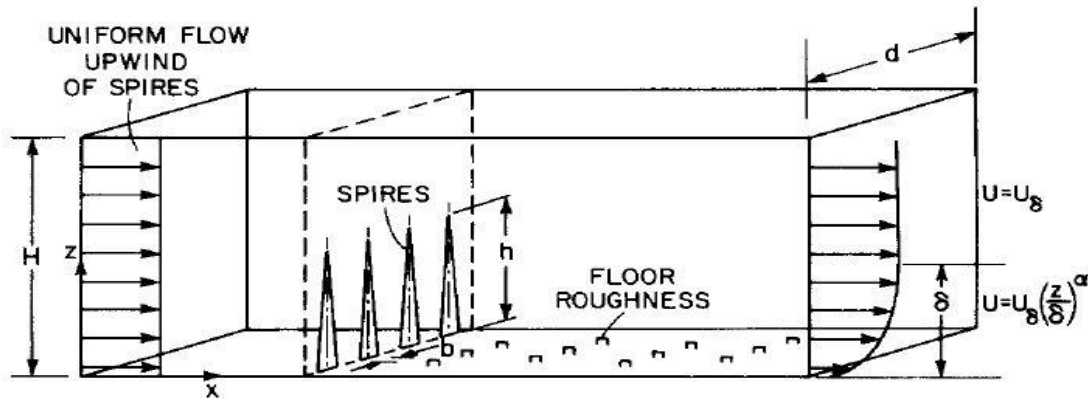


Figure 3.1: Irwin arrangements in Wind Tunnel

Cermak (1984) studied that if wind tunnel has large test -section ($>15\text{m}$) it can generate sufficient thickness of boundary layer around 0.5m to 1m at 10m/s. if test section is small ($<5\text{m}$) is called SBLWT but majority WT is neither LBLWT nor SBWT which test section length vary 5m to 15m that is insufficient length to simulate ABL naturally, so he used many configuration of triangular spires and barriers to increase the BL.

Cesar Farell, K.S. Iyengar (2005) simulated the ABL in Wind Tunnel using spires and barrier wall, and produced the boundary layer which characteristic same as urban terrain condition and they compared the ABL data and experimentally data as turbulence intensity and velocity profiles. For this experiment they used quarter elliptical generator with height $H = 1.2\text{m}$ and

roughness length was 12 m which having 28 mm cube and spacing was 100 mm c/c. They assumed $\alpha=.28$ for urban terrain.

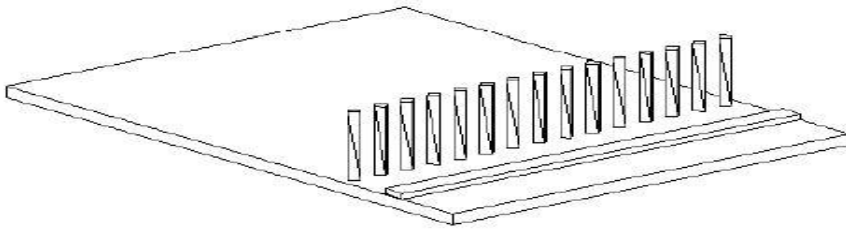


Figure 3.2: Arrangement of array of cylindrical rods and on rectangular bar

Guimaraes et al. (2010) simply used cylindrical, rectangular rods and combinations of spires to increase the BL in WT. He gave 5 different methods and by these methods BL thickness increased by 9 to 18 cm. Rectangular bars used as trip in downstream side. In fig.no.3.2. It is shown 80mm cylindrical rods which spacing is 10 mm and configured in an array across the all width of WT. Blockage area should be less than 5%.

CHAPTER 4: EXPERIMENTAL SETUP AND METHODOLOGY

4.1 GENERAL

Generally length of test section of Wind Tunnel is insufficient for development high scale turbulence intensity and boundary layer depth. To increase the turbulence intensity and boundary layer many passive devices like vortex generator spires and roughness blocks are used by many researcher. In this experimental work we will able to know how different configurations of spires and roughness blocks effects on boundary layer parameter and flow characteristics in test section and establishment of correlation between boundary layer parameters and system variables

4.2 WIND TUNNEL USED FOR EXPERIMENT:

Low speed type Wind Tunnel used in this work. It is built in Hydraulic Machine Laboratory of NIT .Rourkela India and wind speed vary from 6m/s to 25m/s. Wind tunnel consists three parts. These are effuser, working section and diffuser. Effuser is built in upstream side of working section and it is converging cone shape. Working section is built in middle part and here variations in free stream velocity is very less approximately main stream velocity become constant. It is only use for model test. All components size are given in table.no 4.2.

4.2.1 DRIVING UNIT:

Power is supplied continuously to maintain the flow through suction. There is a gear box system in the driving unit of the wind tunnel. As much the requirement of the velocity we want for the experiment, provides by the motor. This is done using a fan or propeller and a motor.

Table 4.1: Wind tunnel specifications

Components	Length(m)	Inlet (m)	Outlet(m)
Effuser	1.4	2.1x2.1	2.1x2.1
Test -section	8	0.6x0.6	0.6x0.6
Diffuser	5	0.6	0.6



Figure 4.1: Wind tunnel at NIT Rourkela

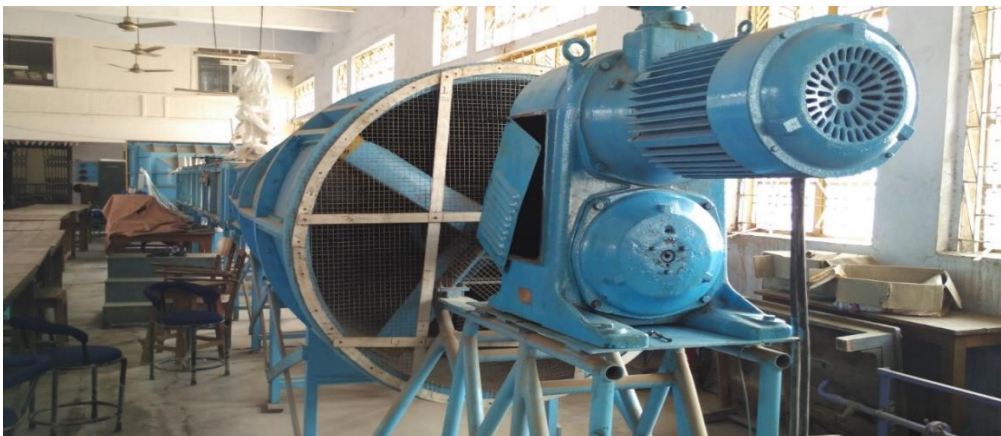


Figure 4.2: Driving unit of Wind Tunnel

4.3 EQUIPMENTS:

For carried out this experiment different type equipment are used which are mention below

1. Telescopic probe velocity meter
2. Digital velocity calico model A00TSI
3. Tachometer
4. Trolley arrangement
5. Spires and 1inch square roughness blocks

4.3.1 TELESCOPIC PROBE VELOCITY METER:

It is sensor type velocity measurement device and it also measure pressure at specific point as well as flow rate. Using procedure is very easy and its error is very less. Its sensor should be parallel to flow direction otherwise it will give wrong value. It can measure velocity in normal direction of the surface in wind tunnel.



Figure 4.3: Digital velocity meter

4.3.2 DIGITAL VELOCIMETER CALICO MODEL A00TSI:

This is digital device which look like calculator which can connect to probe velocity meter and directly get velocity at any point. It work with help of battery and also electricity and we can save our data in this device. It is shown in fig no 4.3.2.



Figure 4.4: Digital velocity meter

4.3.3 TACHOMETER:

The device is being used for the assistance in measuring the rotations per minute of the shaft in the driving unit of the wind tunnel. These records of making changes in the speed of wind tunnel are required because for each grades of plate, the same free stream velocities are to be set. Therefore the work goes on easier if the rpm values are recorded. The tachometer used in the laboratory is fig



Figure 4.5: Tachometer

4.3.4 TROLLEY:

To find the velocity profile at different section in wind tunnel and for the movement of velocity probe meter in different section use trolley which is situated at the top of wind tunnel and velocity meter is connected with trolley, by the help of trolley it is easy to find the velocity at different sections in wind tunnel.



Figure 4.6: Trolley Arrangement

4.3.5 ROUGHNESS SQAURE BLOCKS:

In this experiment 1 inch square blocks are placed over 4feet long wood plate and spacing between blocks are 5cm. Blocks arranged over the plate in two different pattern first is square pattern and second is diamond pattern, cube blocks are rotated 45° from the axis.



Figure 4.7: Square pattern of 1 inch cube blocks



Figure 4.8: Diamond pattern 1 inch cube blocks

4.3.6 SPIRES AREENGMENT:

In upstream of wind tunnel place triangular spires which height is 45cm and base width is 7cm and arranged in an array and spacing's are 6cm, 12cm and 18cm shown in fig no 4.3.6 (a),(b)and (c)



Figure 4.9: Spires with 18cm and 6 spacing respectively



Figure 4.10: Spires with 18cm spacing

4.3.7 COMBINATION OF SPIRES WITH ROUGHNESS BLOCKS:

Spires and blocks are arranged in wind tunnel. Roughness blocks plate are placed 0.5m distance from the spires in wind tunnel. Roughness block plate is placed after the spires, which is shown in figure spires with diamond structure



Figure 4.11: Spires with diamond and square arrangement of cube blocks

4.4 SET-UP

- I. First telescopic probe velocity meter connected to the trolley's arm and made arrangement test section of Wind Tunnel.
- II. Telescopic probe meter placed in the test section of wind tunnel which is built in middle part of Wind Tunnel and trolley can move probe meter at different sections in test section
- III. Velocity probe meter should be parallel to fluid flow. Otherwise its sensor cannot read properly.
- IV. Main part in wind tunnel is test section which is use for model testing because of constant free stream velocity. To analyze the effect on different arrangements of spires and blocks, are placed in test section. It is shown in above figures.
- V. In spire with block arrangement both is placed in test section, in upstream side spires placed than 0.5m from the arrangement of spires roughness wood plate is fixed in test section.
- VI. Five section is located from the end point of roughness plate in test section. At these place with help of trolley we can measure velocity profiles at different speed.



Figure 4.12: Test section of NITRKL Wind Tunnel

4.5 METHODOLOGY

1. First by using tachometer for desired rpms, free stream velocities were measured in test section and results are 760rpm for 7.67m/s, 900rpm for 9.32m/s and 1050rpm for 11.19m/s.
2. Velocity was measured by digital velocity meter in empty test section of wind tunnel at 27°C inside the test section.
3. 4 feet long roughness wood plate fixed in test section with the help of screws and five sections are marked in test section from end point of roughness block plate and these distance are 20cm, 40cm, 60cm, 80cm, and 100cm from end point of roughness plate.
4. In each section velocity profile is measured by digital velocity meter. Velocity profiles is measured by 4mm intervals but later it increased by 10mm interval in perpendicular y direction from surface of the Wind Tunnel.
5. First for blocks arrangements velocity profiles was measured at all 5 marked section in test section at desired free stream velocities again only for spires with varying spacing velocity profiles were measured at same sections.
6. For spires with blocks arrangement above procedure has been followed and velocity profiles were measured at same five sections for same main stream velocities.
7. This experiment was done for three different constant free-stream velocities; viz. 6.67m/s, 9.32m/s and 11.19m/s. then the tabulated data were supposed to be used for plot of graphs and further observations.

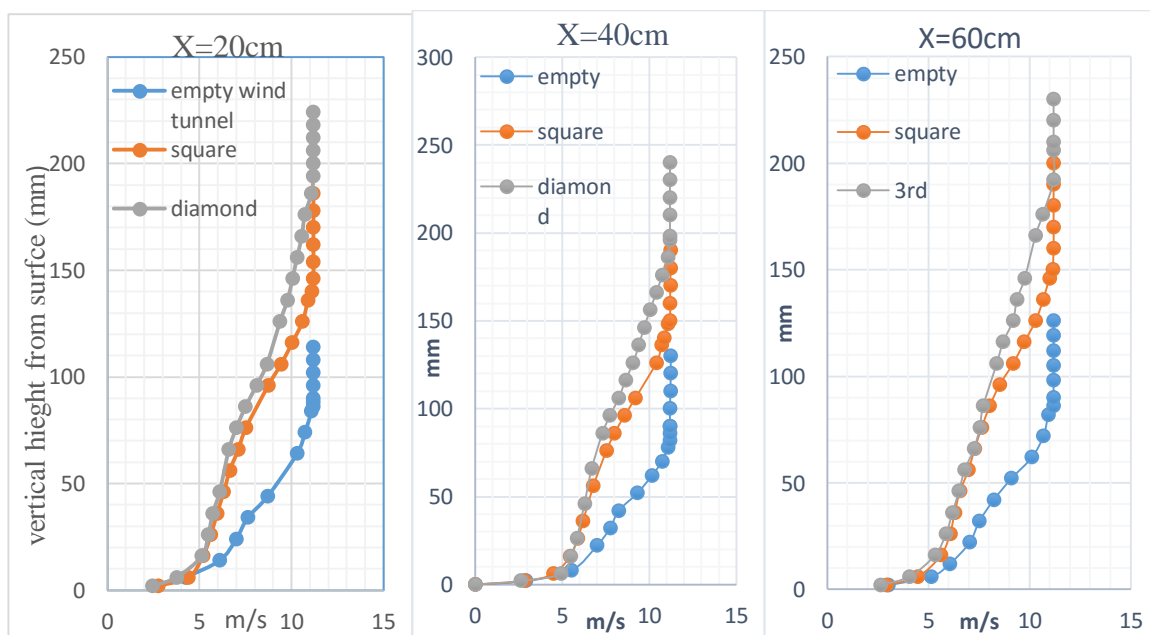
CHAPTER 5: RESULTS AND DISCUSSION

5.1 OVERVIEW

Methodology and experimental set-up has been described in previous chapter. This chapter consists results and discussion parts of the experimental work. The results are about variation in velocity profiles and boundary layer in test section with respect to free stream velocities and all roughness arrangements. Boundary layer thickness in test section are plotted at desired free stream velocities. Mainly graphs are presented here as a results and graphs are-

- Between v vs. y graphs are plotted at different free stream velocity from experimental data at different sections in wind tunnel.
- Velocity profiles for all arrangements at constant free stream velocity are plotted.
- Boundary layer thickness for all arrangements of spires and blocks represented as graphs in y direction and longitudinal distance in wind tunnel in x direction..

5.2 VELOCITY PROFILES FOR DIFFERENT ARRANGEMENTS OF BLOCKS



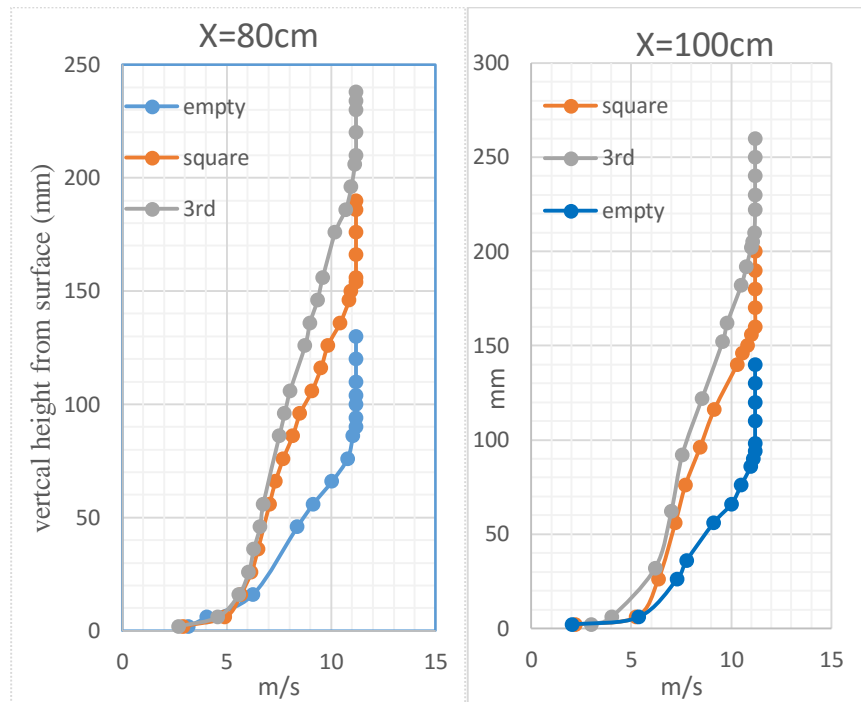
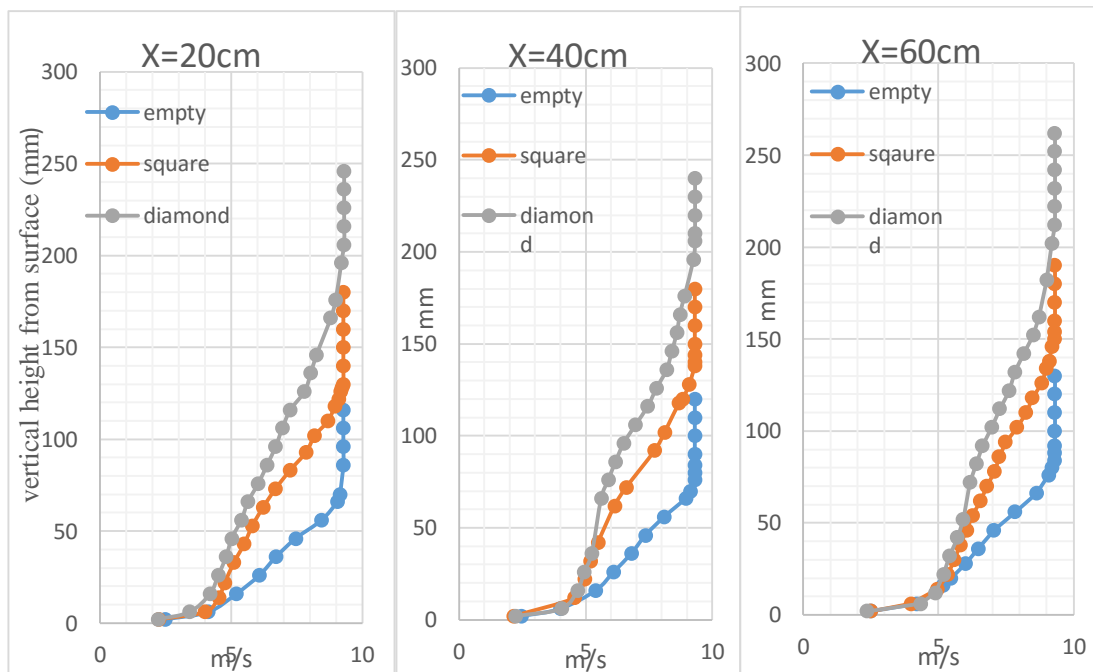


Figure 5.1: Velocity profiles for different arrangements of blocks at $V=11.19\text{m/s}$



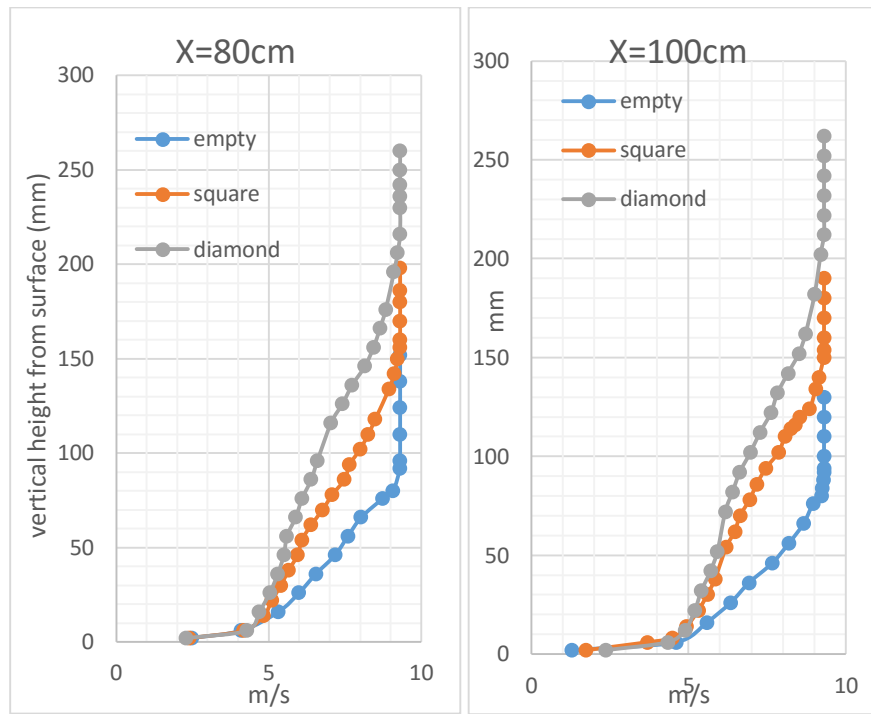
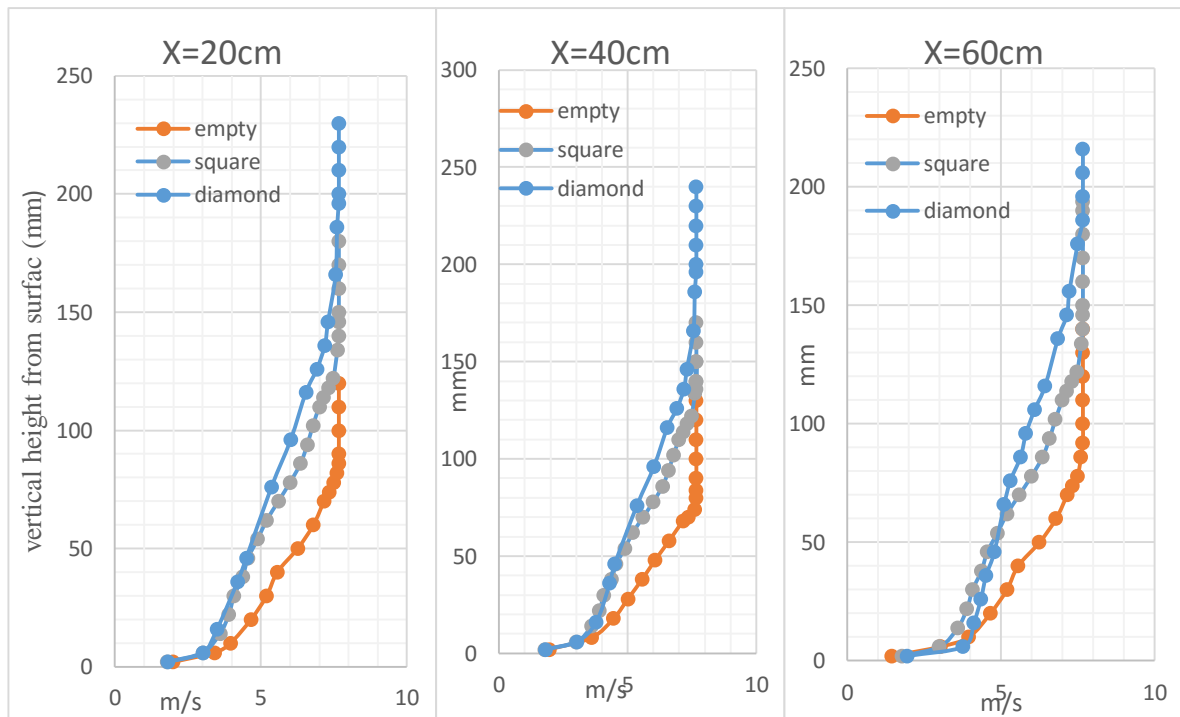


Figure 5.2: velocity profiles for different arrangements of blocks at $V=9.32\text{ m/s}$



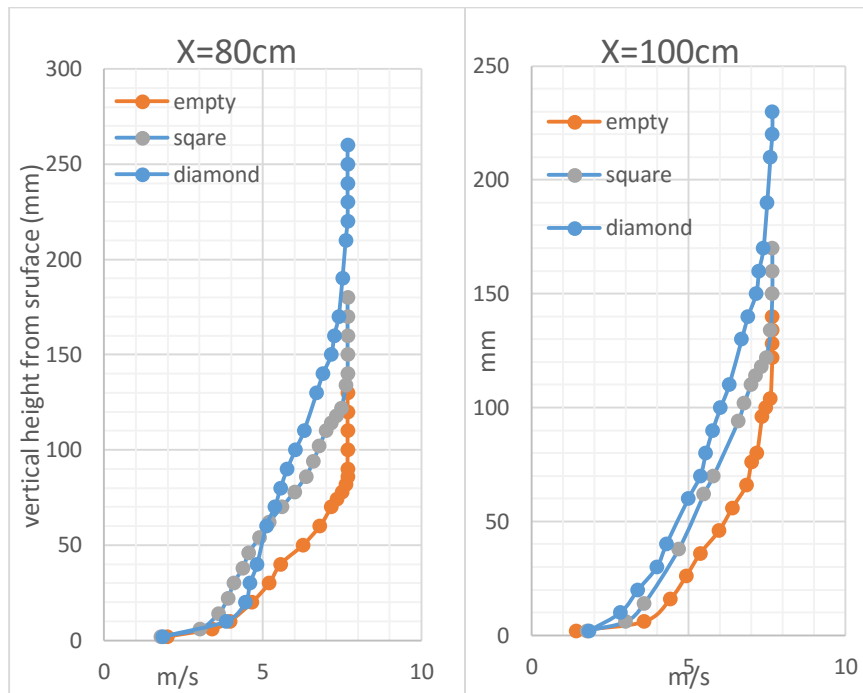
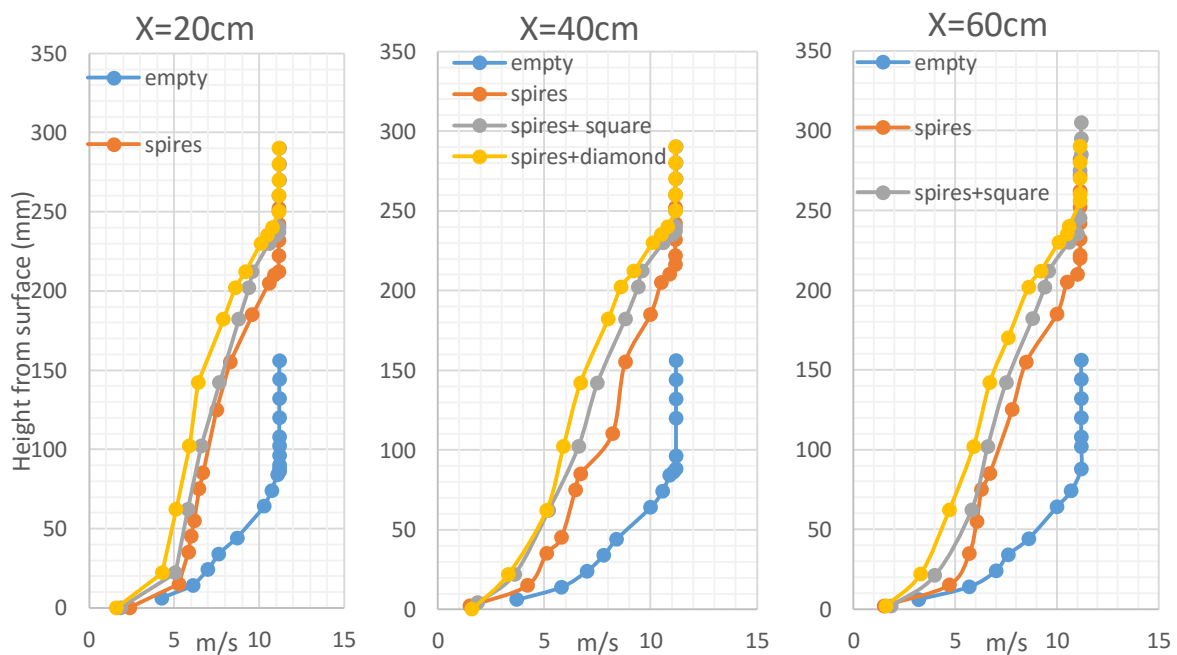


Figure 5.3: velocity profiles for different arrangements of blocks at $V=7.67\text{m/s}$

5.3 VELOCITY PROFILES FOR DIFFERENT ARRANGEMENTS OF SPIRES AND BLOCKS AT CONSTANT FREE STREAM VELOCITY:



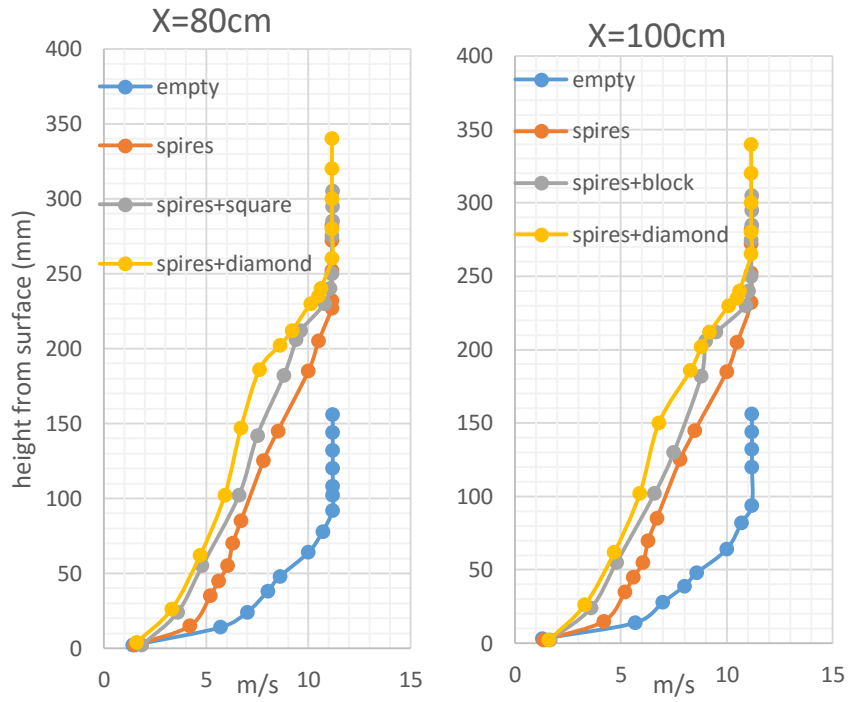


Figure 5.4: velocity profiles at $V=11.19\text{m/s}$

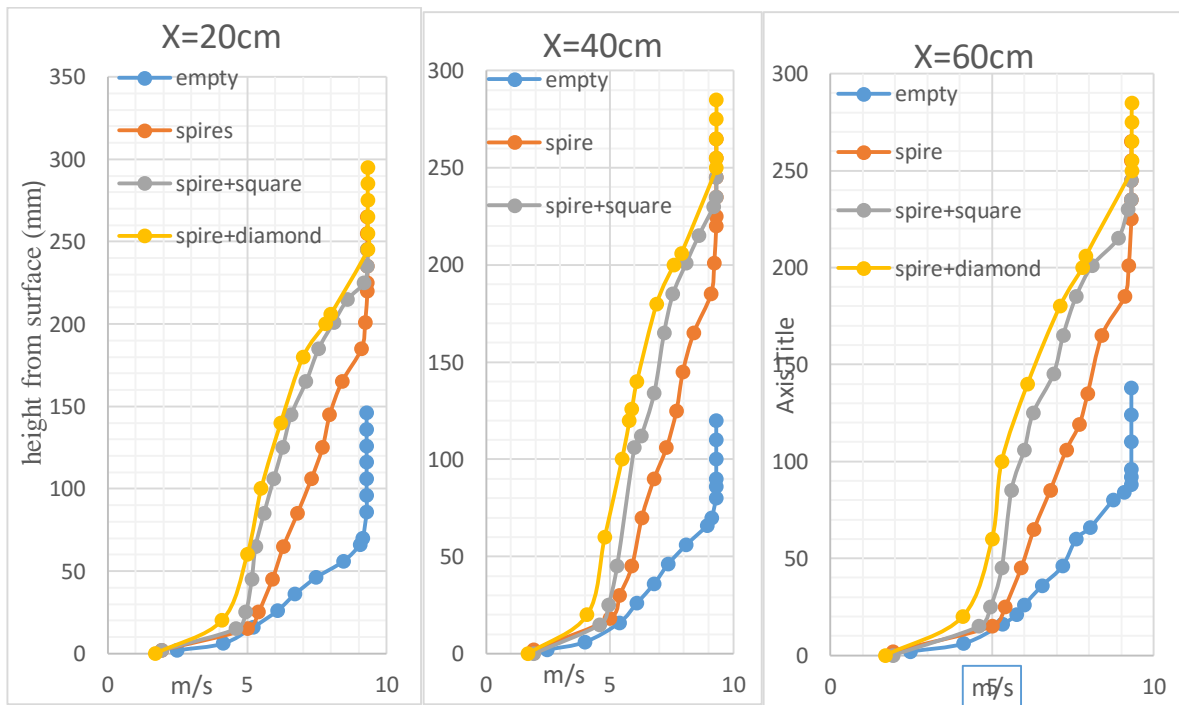


Figure 5.5: velocity profiles at $V=9.32\text{m/s}$

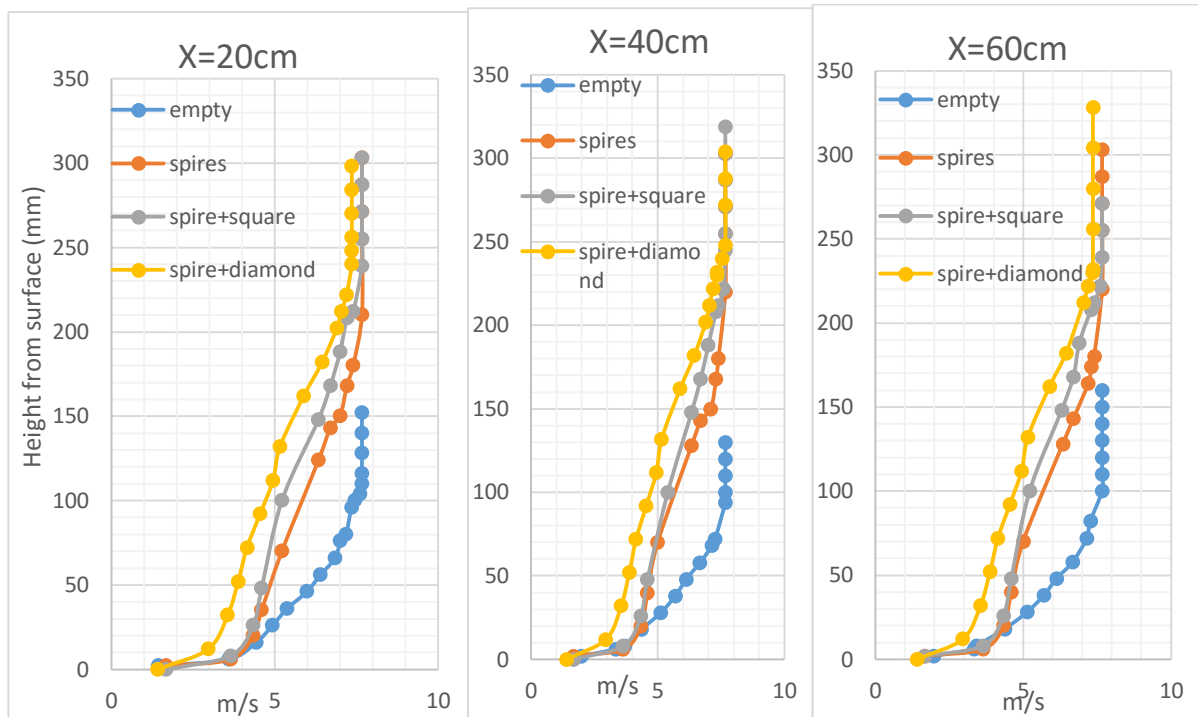


Figure 5.6: velocity profiles at $V=7.67\text{m/s}$

5.4 VARIATIONS IN BOUNDARY LAYER FOR ALL ARRANGMENT AT CONSTANT VELOCITY

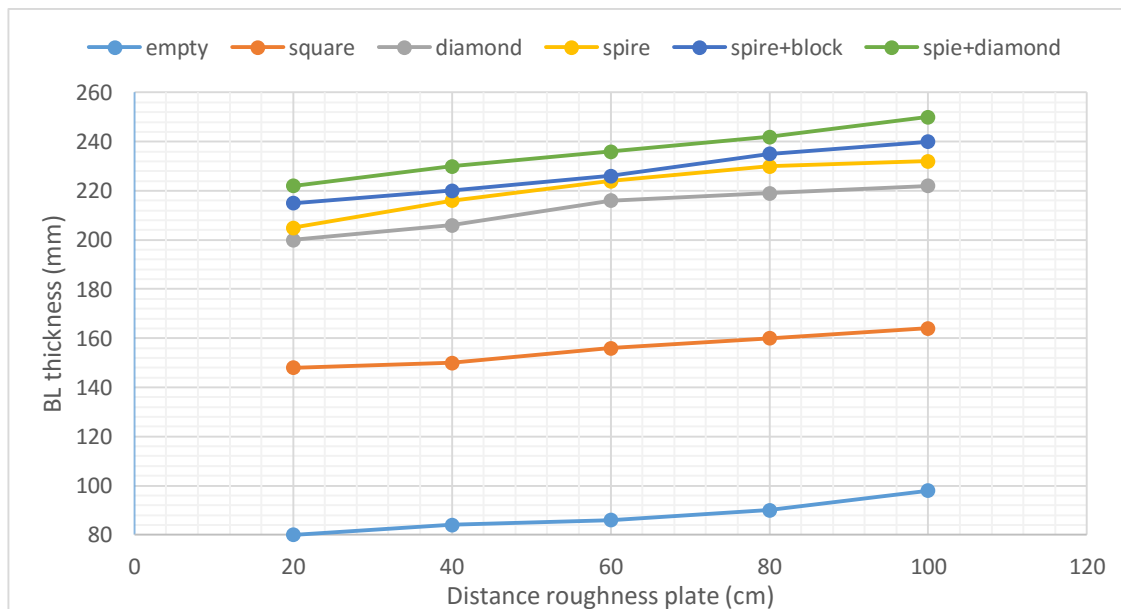


Figure 5.7: Boundary layer thickness at $V=11.31\text{m/s}$

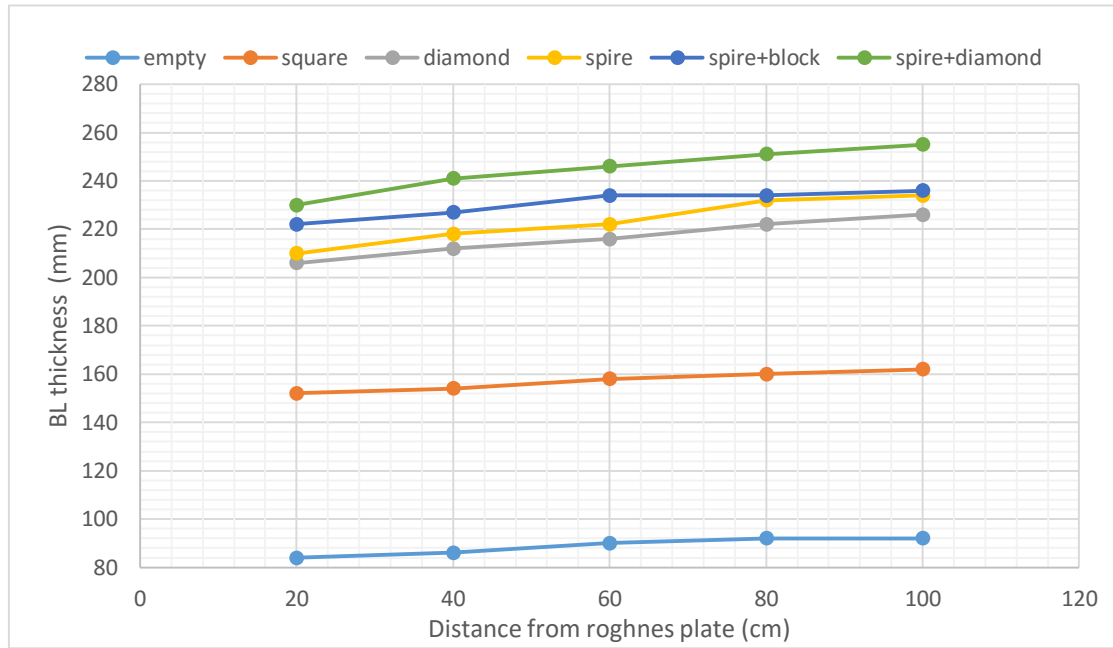


Figure 5.8: Boundary layer thickness at $V=9.32\text{m/s}$

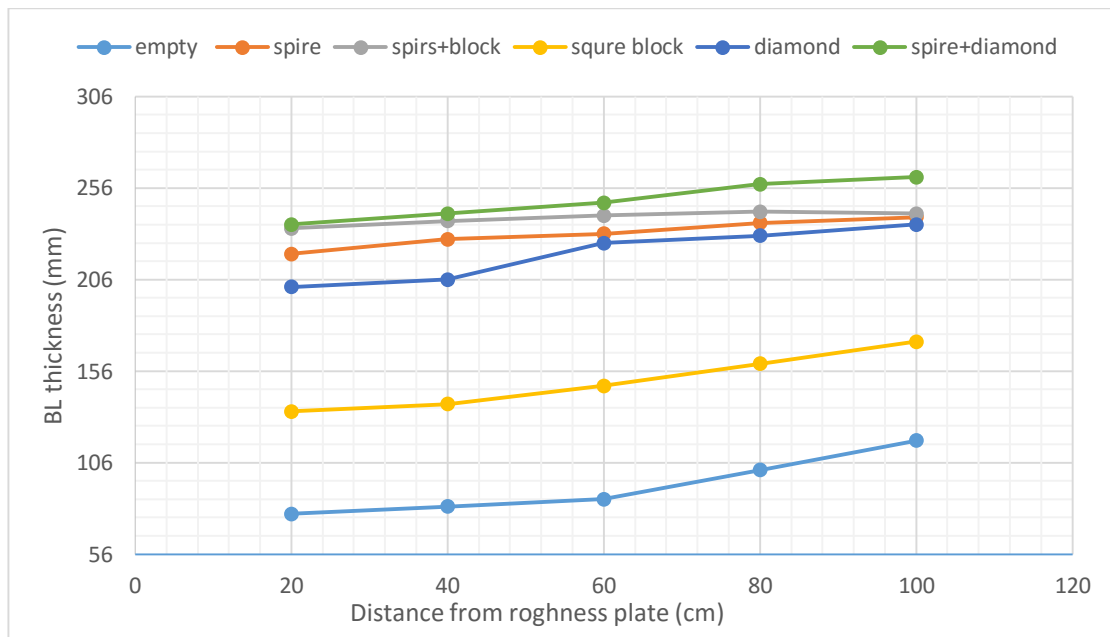


Figure 5.9: Boundary layer thickness at $V=7.67\text{m/s}$

5.5 VARIATION IN BOUBADRY LAYER FOR SAME ARRANGEMENT AT VARYING FREE STREAM VELOCITIES:

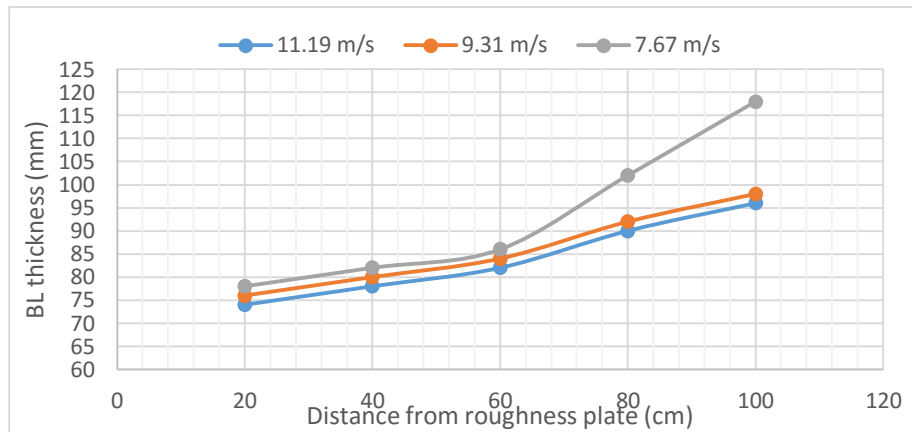


Figure 5.10: BL thickness for empty Wind Tunnel

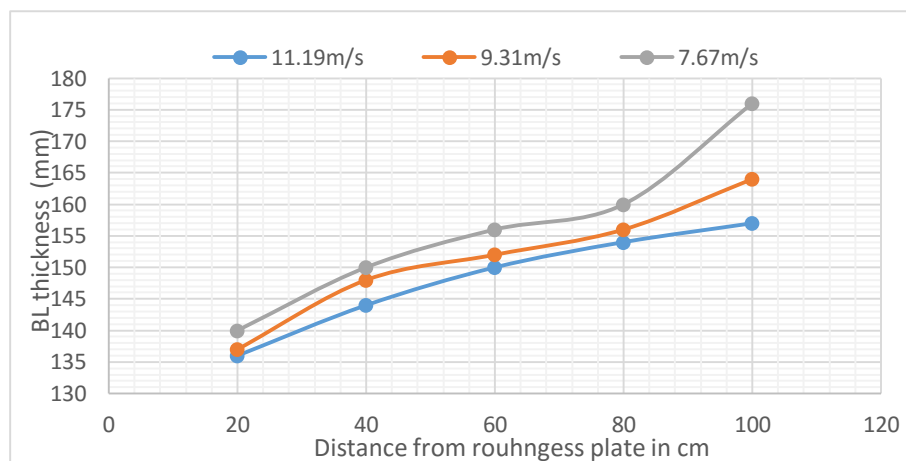


Figure 5.11: BL thickness for square pattern of blocks

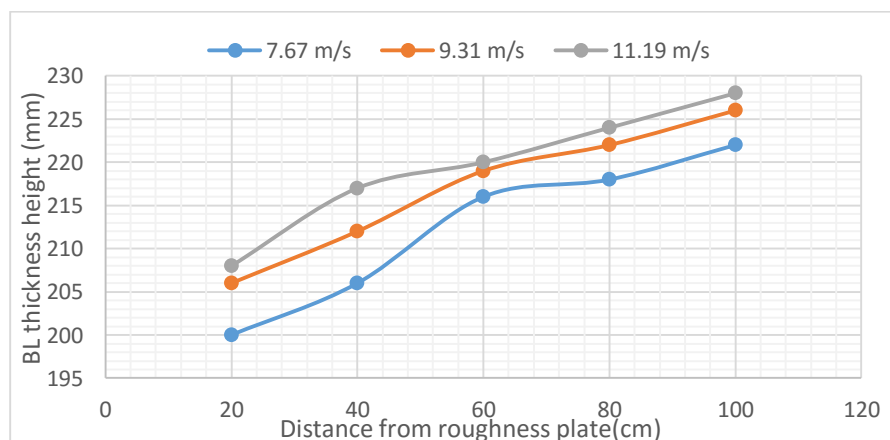


Figure 5.12: BL thickness for diamond pattern of blocks

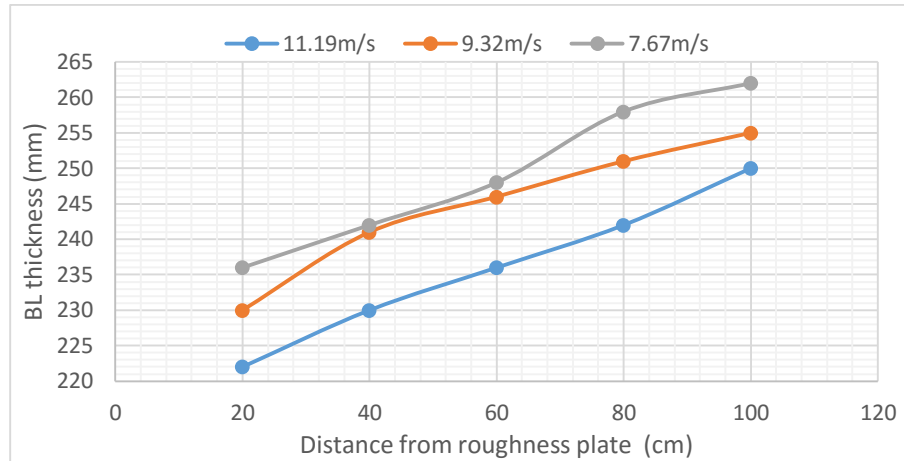


Figure 5.13: Boundary layer variation for spire with diamond configuration of blocks

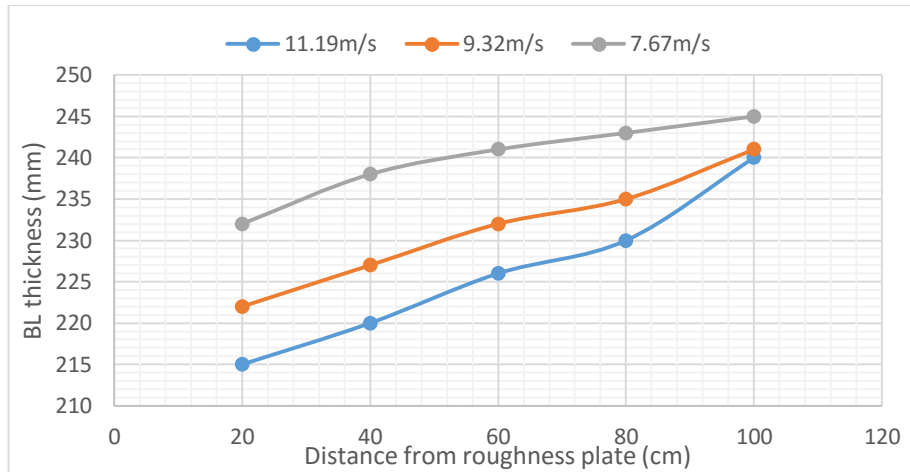


Figure 5.14: Boundary layer variation for spires with square configuration of blocks

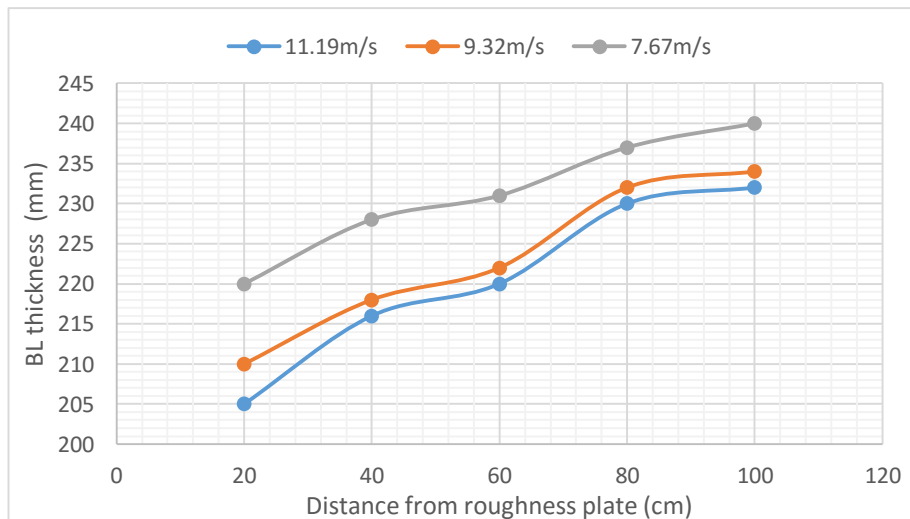


Figure 5.15: Boundary layer variation for spires with 6cm c/c spacing

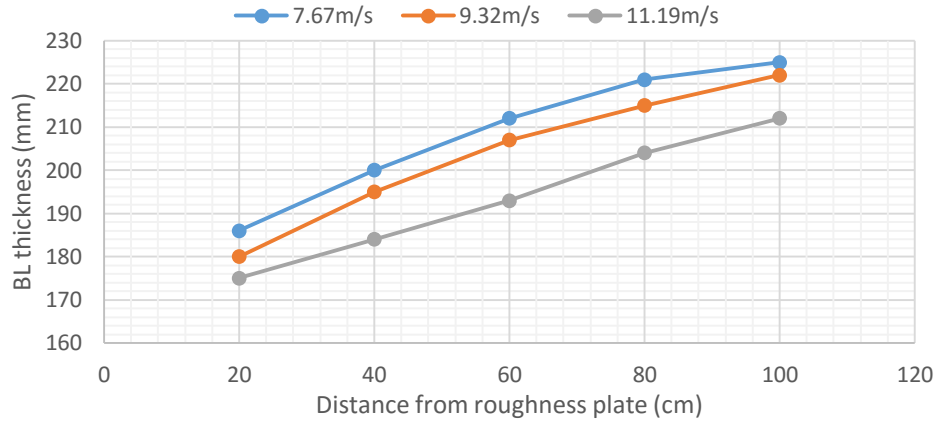


Figure 5.16: Boundary layer variation for spires with 12 cm c/c spacing

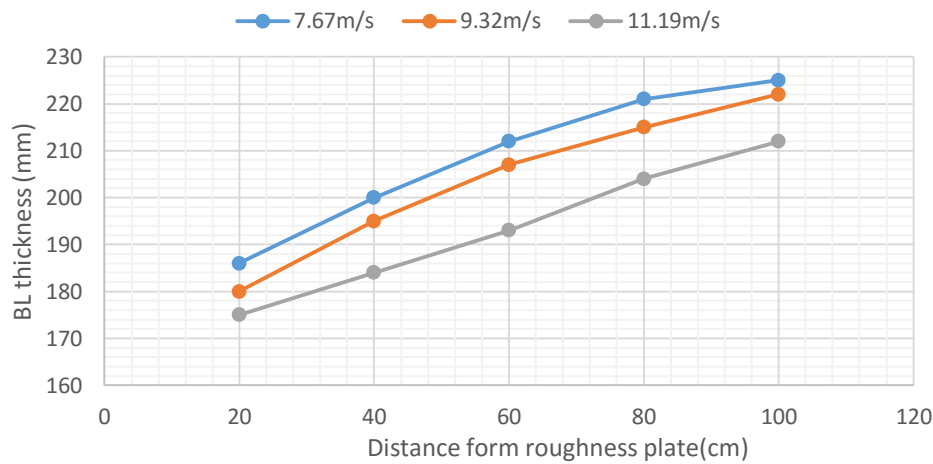


Figure 5.17: Boundary layer variation for spires having c/c spacing 18cm

5.6 ESTIMATION OF ROUGHNESS LENGTH FOR DIFFERENT ARRANGEMENTS

$$U(z) = \frac{u_*}{k} [\ln(z) - \ln(z_0)] \quad \text{Log- law}$$

By log- law z_0 are estimated with the help of graphs $\ln(z)$ vs $U(z)$ and best fitted line equation used for z_0

$$z_0 = e^{\frac{-c}{m}} \quad c \text{ is line intercept}$$

m = slope of line in graph

z = height from the surface

u_* = Friction velocity

$\ln(z)$ vs $U(z)$ For all roughness patterns:

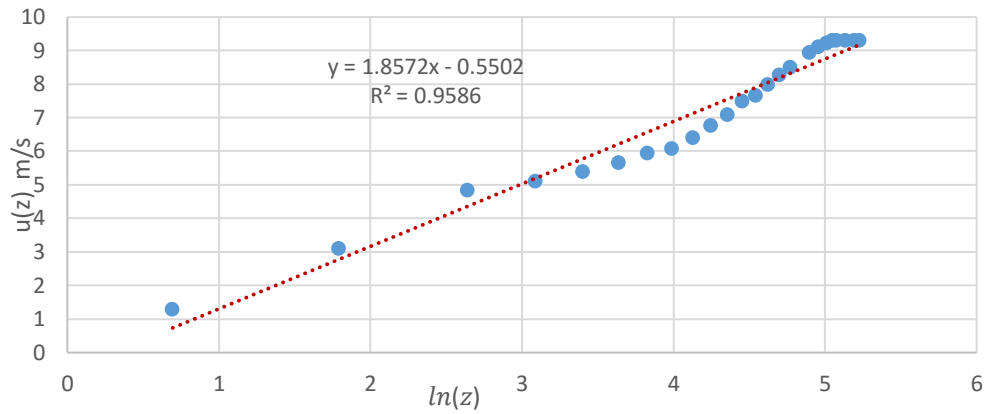


Figure 5.18: Estimation of roughness length for square pattern of blocks

For square pattern best fitted line equation is $y = 1.8572x - 0.5502$ and $R^2 = 0.9586$

Comparison of best fitted line equation and log-law equation

$$U(z) = 1.8572 \ln(z) - 0.5502 \quad \text{From the graph}$$

$$U(z) = \frac{u_*}{k} [\ln(z) - \ln(z_0)] \quad \text{Log- law}$$

$$z_0 = e^{\frac{0.5502}{1.8572}}$$

$$z_0 = 1.357 \text{ mm}$$

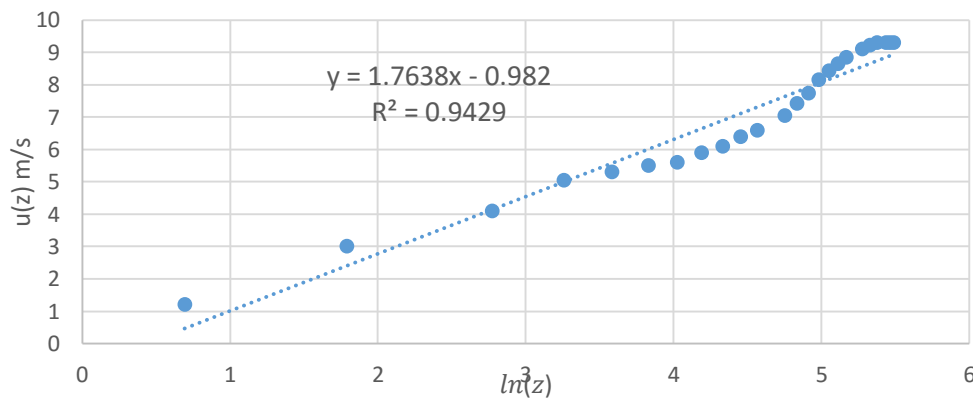


Figure 5.19: Roughness length estimation in WT for diamond pattern of blocks

$$U(z) = 1.7638 \ln(z) - 0.982 \quad \text{From the graph}$$

$$U(z) = \frac{u_*}{k} [\ln(z) - \ln(z_0)] \quad \text{Log- law}$$

$$Z_0 = e^{\frac{0.982}{1.7638}}$$

$$Z_0 = 1.745 \text{ mm}$$

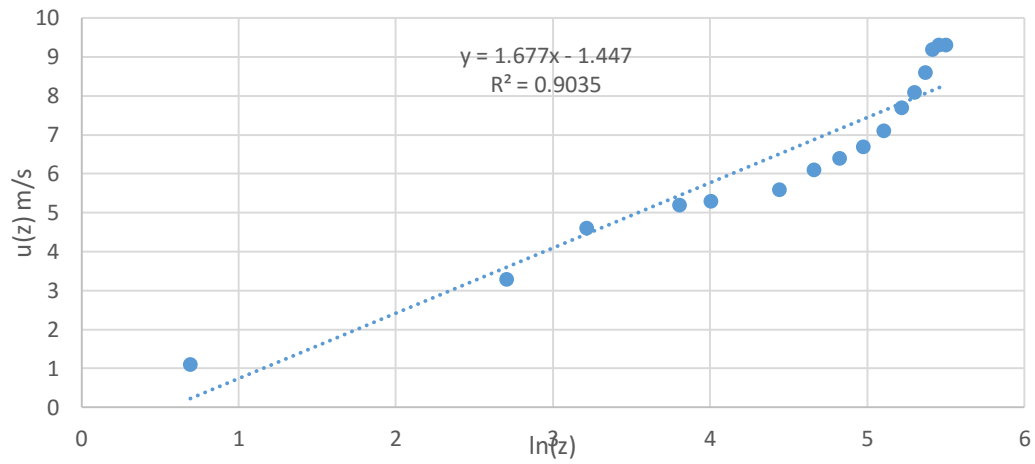


Figure 5.20: Roughness length estimation for spires with square pattern of blocks

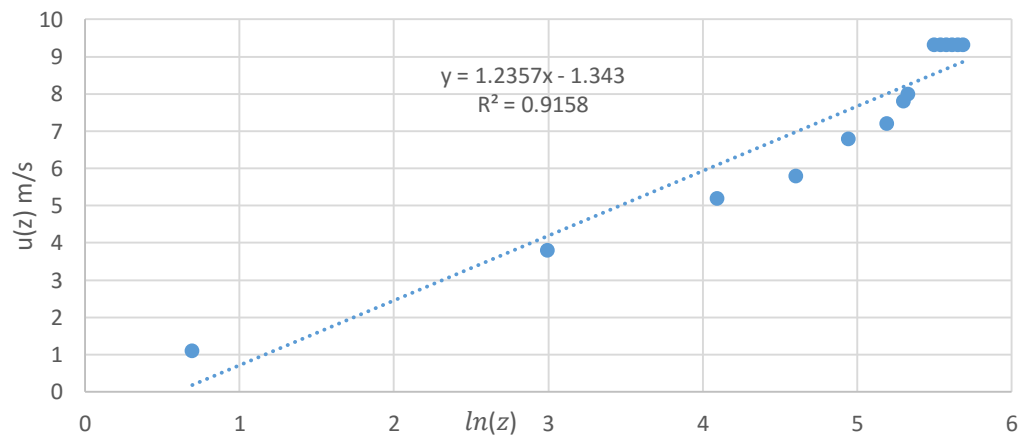


Figure 5.21: Roughness length estimation for spires with diamond pattern of blocks

Table 5.1: Roughness thickness for all configuration

Roughness length from log-law(z_0)	Configurations in WT
1.357mm	Square pattern of blocks
1.745mm	Diamond pattern of blocks
2.367mm	Spires with square pattern of blocks
3.056mm	Spires with diamond pattern of blocks

5.7 CALCULATIONS OF PARAMETERS OF BOUNDARY LAYER:

5.7.1 Calculations method of boundary layer parameters:

From graph $\frac{y}{\delta}$ vs $\frac{v}{V}$ obtained best fitted second order polynomial equation in form of $(Ax^2 + Bx + c)$ here,

$$y = Ax^2 + Bx + c \quad \text{From the graphs}$$

$$\frac{v}{V} = A\left(\frac{y}{\delta}\right)^2 + B\left(\frac{y}{\delta}\right) + c$$

$$\begin{aligned} \delta^* &= \int_0^{\delta} \left(1 - \frac{v}{V}\right) dy \\ &= \int_0^{\delta} (1 - (Ax^2 + Bx + c)) dy \end{aligned}$$

$$\begin{aligned} \theta &= \int_0^{\delta} \frac{v}{V} \left(1 - \frac{v}{V}\right) dy \\ &= \int_0^{\delta} (Ax^2 + Bx + c)(1 - (Ax^2 + Bx + c)) dy \end{aligned}$$

(a) $\frac{y}{\delta}$ vs $\frac{v}{V}$ Graph for square pattern blocks at $V=7.67$ m, $x=20$ cm from roughness plate

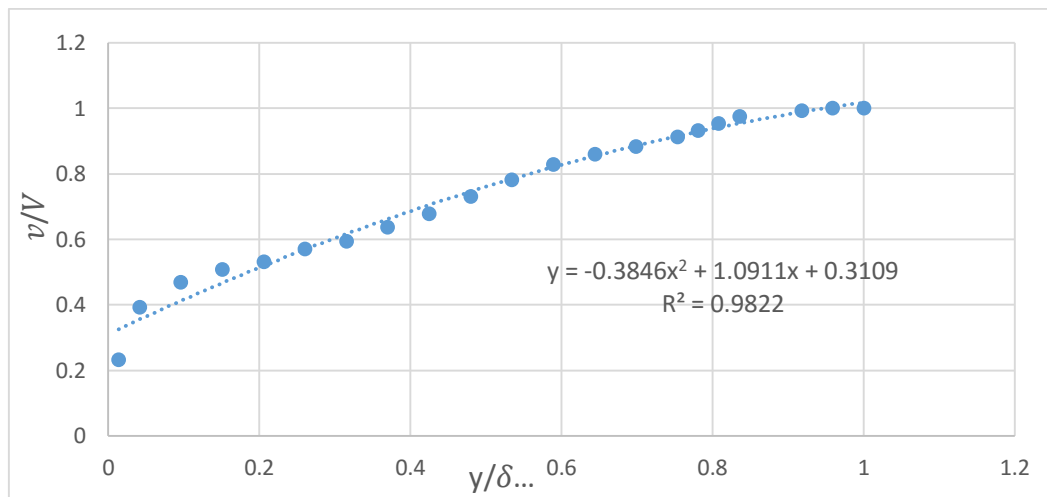


Figure 5.22: Graph for square pattern blocks at $V=7.67$ m, $x=20$ cm from roughness plate

$$\frac{v}{V} = -0.3846\left(\frac{y}{\delta}\right)^2 + 1.0911\frac{y}{\delta} + 0.3109,$$

$$\delta^* = 39.22\text{mm}, \quad \theta = 19.344\text{mm}$$

(b) $\frac{v}{\delta}$ vs $\frac{v}{V}$ Graph for diamond pattern of blocks at $V=7.67$ m, $x=20$ cm from roughness plate:

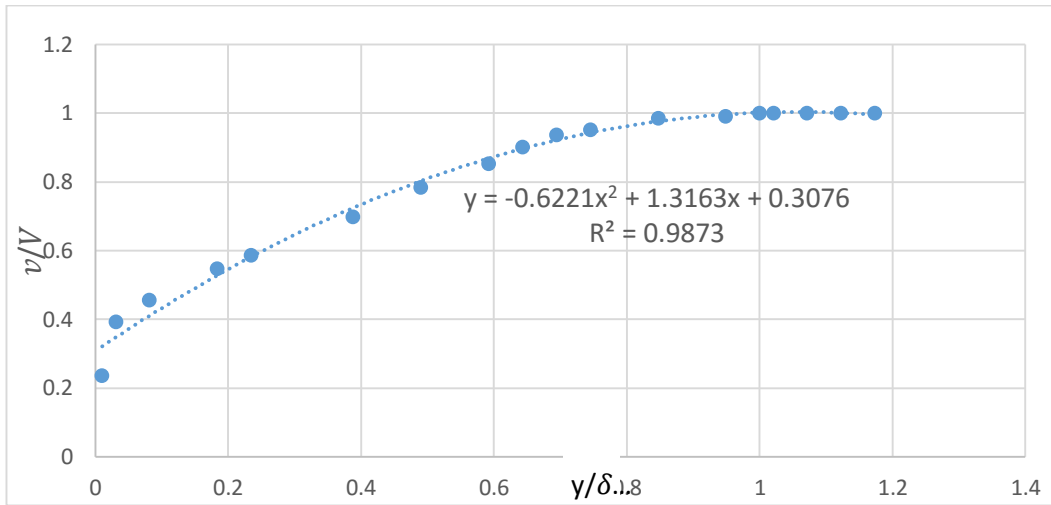


Figure 5.23: Graph for diamond pattern of blocks at $V=7.67$ m, $x=20$ cm from roughness plate

$$\frac{v}{V} = -0.622 \left(\frac{y}{\delta} \right)^2 + 1.3163 \frac{y}{\delta} + 0.3076 \quad \text{From above fig}$$

$$\delta^* = 50.1\text{mm}, \quad \theta = 28.22\text{mm}$$

(c) $\frac{v}{\delta}$ vs $\frac{v}{V}$ Graph for diamond pattern of blocks at $V=9.31$ m/s, $x=20$ cm from roughness plate

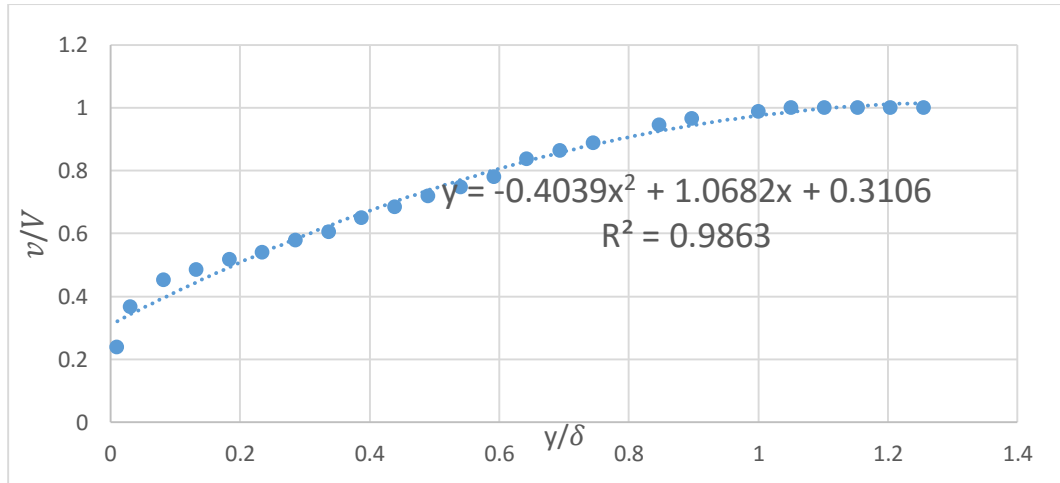


Figure 5.24: Graph for diamond pattern of blocks at $V=9.31$ m/s, $x=20$ cm from roughness plate

$$\frac{v}{V} = -0.4039 \left(\frac{y}{\delta} \right)^2 + 1.0682 \frac{y}{\delta} + 0.3106 \quad \text{From the fig}$$

$$\delta^* = 53.4\text{mm}, \quad \theta = 31.96\text{mm}$$

(d) $\frac{y}{\delta}$ vs $\frac{v}{V}$ Graph for diamond pattern of blocks at V=9.32m/s, x=60 cm from roughness plate:

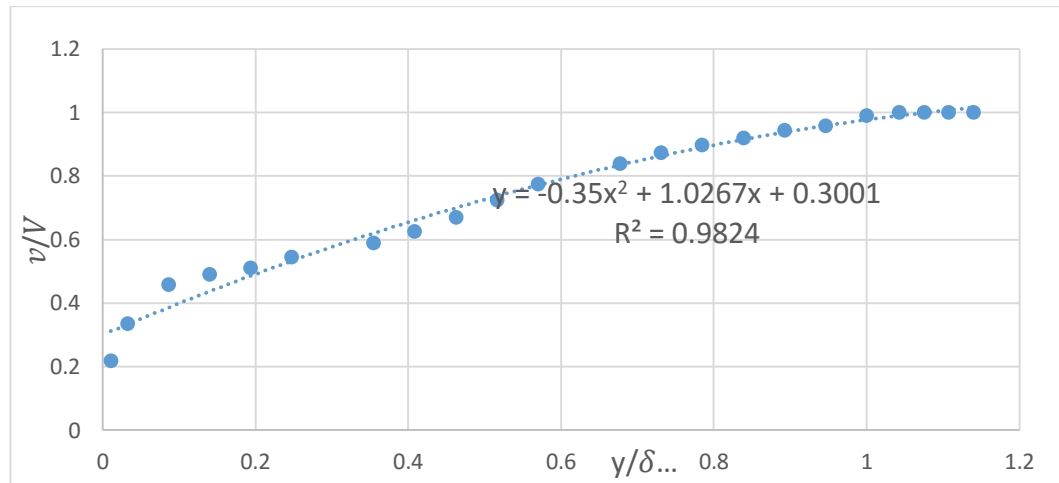


Figure 5.25: Graph for diamond pattern of blocks at V=9.32m/s, x=60 cm from roughness plate

From above graph-

$$\frac{v}{V} = -0.35 \left(\frac{y}{\delta} \right)^2 + 1.0267 \frac{y}{\delta} + 0.3001$$

$$\delta^* = 56.46\text{mm} \quad , \quad \theta = 34.11\text{mm}$$

(e) $\frac{y}{\delta}$ vs $\frac{v}{V}$ Graph for square pattern of blocks at V=11.19m/s, x=20cm from roughness plate:

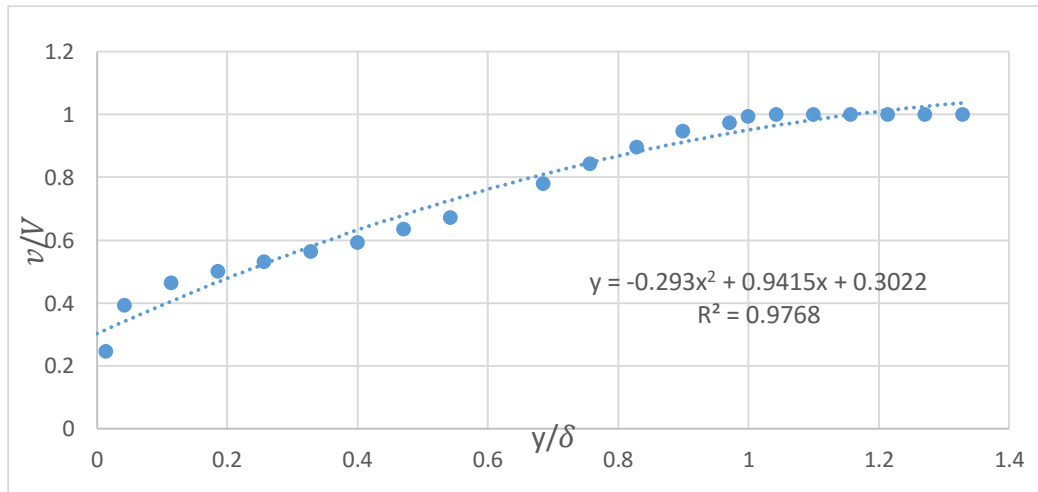


Figure 5.26: Graph for square pattern of blocks at V=11.19m/s, x=20cm from roughness plate:

$$\frac{v}{V} = -0.293 \left(\frac{y}{\delta} \right)^2 + 0.9415 \frac{y}{\delta} + 0.3022$$

$$\delta^* = 44.6\text{mm} \quad , \quad \theta = 26.266\text{mm}$$

(f) $\frac{y}{\delta}$ vs $\frac{v}{V}$ Graph for spires with diamond pattern of blocks at $V=11.19\text{m/s}$, $x=20\text{cm}$ from roughness plate

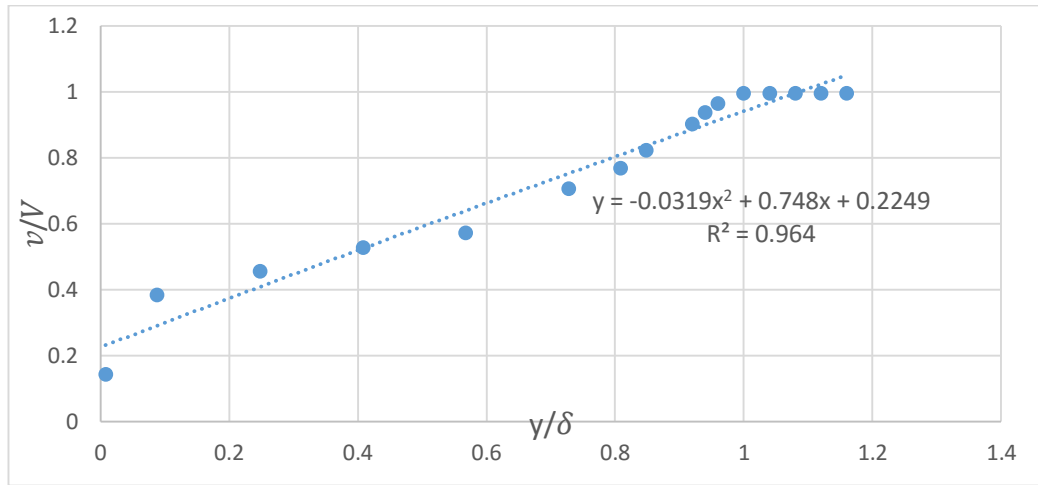


Figure 5.27: Graph for spires with diamond pattern of blocks at $V=11.19\text{m/s}$, $x=20\text{cm}$ from roughness plate

$$\frac{v}{V} = -0.0319 \left(\frac{y}{\delta} \right)^2 + 0.748 \frac{y}{\delta} + 0.2249$$

$$\delta^* = 109\text{mm}, \theta = 49.53\text{mm}$$

(g) $\frac{y}{\delta}$ vs $\frac{v}{V}$ Graph for spire with square pattern of blocks at $V=11.19\text{m/s}$, $x=20\text{cm}$ from roughness plate

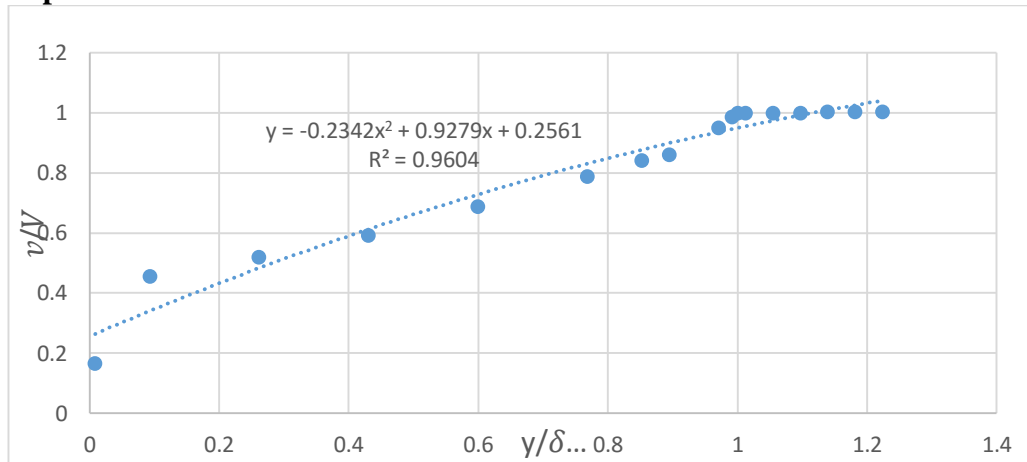


Figure 5.28: Graph for spire with square pattern of blocks at $V=11.19\text{m/s}$, $x=20\text{cm}$ from roughness plate

$$\frac{v}{V} = -0.234 \left(\frac{y}{\delta} \right)^2 + 0.9278 \frac{y}{\delta} + 0.2561$$

$$\delta^* = 84.83\text{mm}, \theta = 38.9\text{mm}$$

(h) $\frac{y}{\delta}$ vs $\frac{v}{V}$ Graph for spire with diamond pattern of blocks at $V=9.31\text{m/s}$, $x=20\text{cm}$

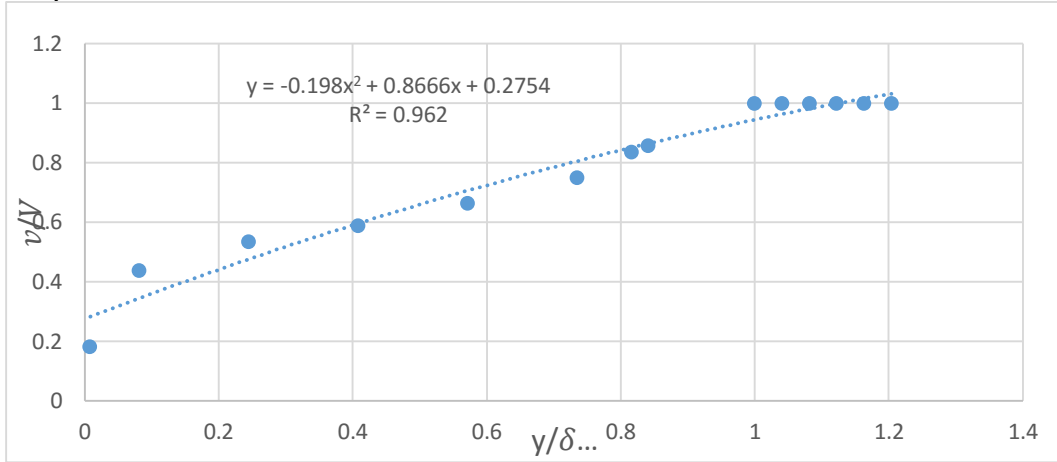


Figure 5.29: Graph for spire with diamond pattern of blocks at $V=9.31\text{m/s}$, $x=20\text{cm}$

$$\frac{v}{V} = -0.198 \left(\frac{y}{\delta} \right)^2 + 0.866 \frac{y}{\delta} + 0.2754$$

$$\delta^* = 90.2\text{mm}, \quad \theta = 39.67\text{mm}$$

(I) $\frac{y}{\delta}$ vs $\frac{v}{V}$ Graph for spire with square pattern of blocks at $V=9.31\text{m/s}$, $x=20\text{cm}$ from trailing edge

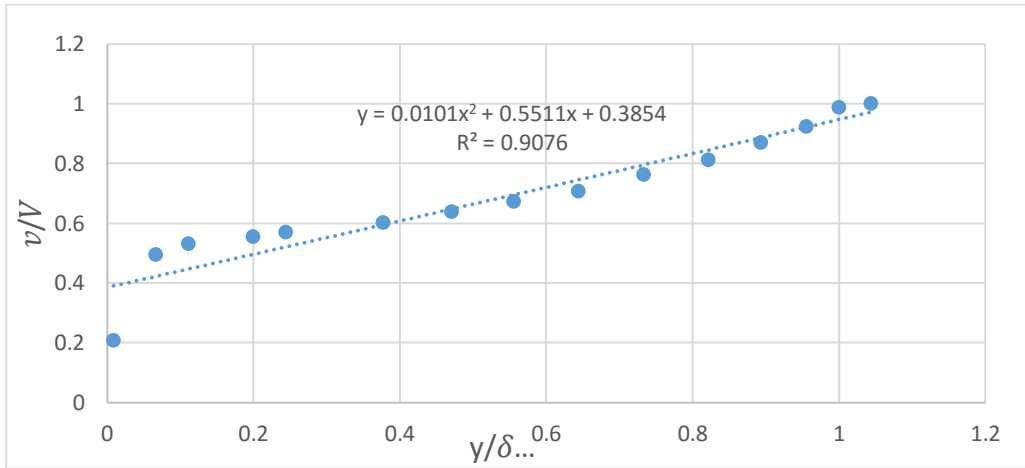


Figure 5.30: Graph for spire with square pattern of blocks at $V=9.31\text{m/s}$, $x=20\text{cm}$ from trailing edge

From the graph we get

$$\frac{v}{V} = -0.0101 \left(\frac{y}{\delta} \right)^2 + 0.551 \frac{y}{\delta} + 0.3854$$

$$\delta^* = 76.3\text{mm},$$

$$\theta = 35.3$$

(j) $\frac{y}{\delta}$ vs $\frac{v}{V}$ Graph for spire with diamond pattern of blocks at $V=7.67\text{m/s}$, $x=20\text{cm}$ from roughness plate-

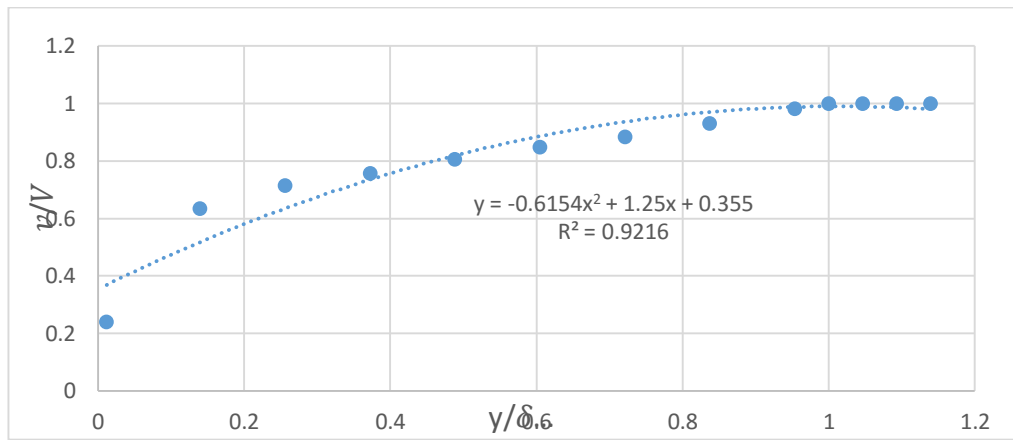


Figure 5.31: Graph for spire with diamond pattern of blocks at $V=7.67\text{m/s}$, $x=20\text{cm}$ from roughness plate

From the above graph $\frac{v}{V} = -0.6154 \left(\frac{y}{\delta} \right)^2 + 1.25 \frac{y}{\delta} + 0.355$

$$\delta^* = 86.12,$$

$$\theta = 37.4$$

(k) $\frac{y}{\delta}$ vs $\frac{v}{V}$ Graph for spires with square pattern of blocks at $V=7.67\text{m/s}$, $x=20\text{cm}$ from roughness plate

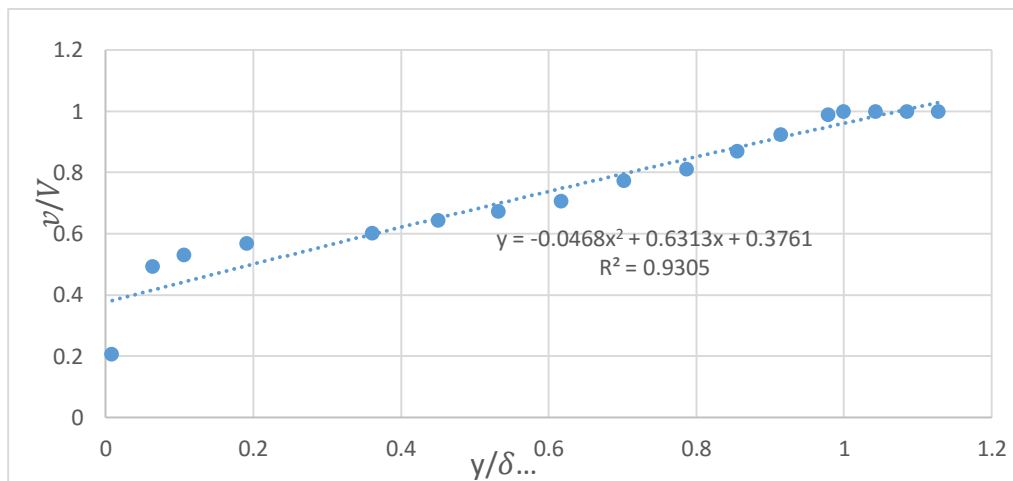


Figure 5.32: Graph for spires with square pattern of blocks at $V=7.67\text{m/s}$, $x=20\text{cm}$ from roughness plate

From the above graph $\frac{v}{V} = -0.0468 \left(\frac{y}{\delta} \right)^2 + 0.6313 \frac{y}{\delta} + 0.3761$

$$\delta^* = 64\text{mm},$$

$$\theta = 33.56\text{mm}$$

Table 5.2: Calculated values of BL parameters with system variables

Roughness (z) mm	Distance from trailing edge (cm)	Velocity (m/s)	BL thickness (mm)	Displacement Thickness (mm)	Momentum thickness (mm)
1.345	20	11.19	134	44.60	26.26
1.745	20	11.19	176	56.46	34.11
2.367	20	11.19	194	84.83	38.90
3.056	20	11.19	235	109.00	49.53
1.345	20	7.67	157	39.22	19.34
1.345	20	9.32	146	43.45	22.29
1.345	20	11.19	134	44.60	26.27
1.745	20	7.67	192	50.10	28.22
1.745	20	9.32	181	53.40	31.96
1.745	20	11.19	176	56.46	32.38
2.367	20	7.67	210	64.00	33.56
2.367	20	9.32	205	76.30	35.30
2.367	20	11.19	194	84.83	38.90
3.056	20	7.67	238	86.12	37.40
3.056	20	9.32	230	90.2.0	39.67
3.056	20	11.19	223	109.00	49.53
3.056	40	11.19	226	111.10	50.01
3.056	60	11.19	231	112.2	51.03
3.056	80	11.19	242	113.34	51.89
3.056	100	11.19	252	114.12	52.20

5.8 CORREALTION OF VARIABLES:

Boundary layer parameters are generally most helpful to study the flow properties of real fluid over the solid surface. From Experimental and calculation value of boundary layer parameters were shown in previous chapter. In this chapter correlation is established using power equations. There are two variable one is dependent and second is independent in this experiment independent variable is system variable like velocity, roughness length and distance from roughness plate which can vary and correlate to the BL parameters.

DEPENDENT VARIABLE-

BL Thickness δ

Displacement thickness δ^*

Momentum thickness θ

Correlation between dependent and independent variable and we can write dependent variable as functions of independent variables.

$$\delta, \delta^*, \theta = f(Z_0, V, X)$$

X= distance from roughness plate in cm

Z_0 = roughness length

V = free stream velocity

$$\delta, \delta^*, \theta = A(z_0)^a (V)^b (X)^c, \text{ a, b, c are exponent}$$

Exponents a, b, and c are determined by Fig no.6.1.1(a) to Fig no. 6.1.3(c) and power equation used in the graphs to correlate each independent variable with dependent variables

And again correlate to whole function as consider one system with boundary layer parameters

$$\delta, \delta^*, \theta = B[(z_0)^a (V)^b (X)^c]^d$$

Exponent d and constant B is determined by Fig no.6.1.1 (d), Fig no. 6.1.2 (d) and Fig no. 6.1.3 (d).to fig no and here all independent variables consider one system and by using power equation correlate..

5.8.1 Exponent's determination for BL thickness (δ):

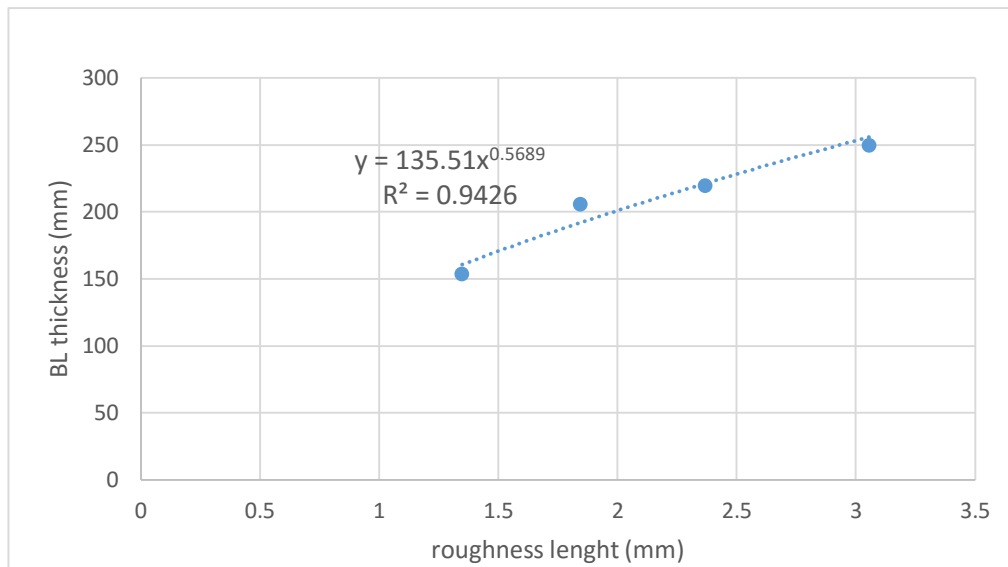


Figure 5.33: Roughness exponent determination for BL thickness

$$\delta = 135.52Z_0^{0.5689}$$

$$a = 0.5689$$

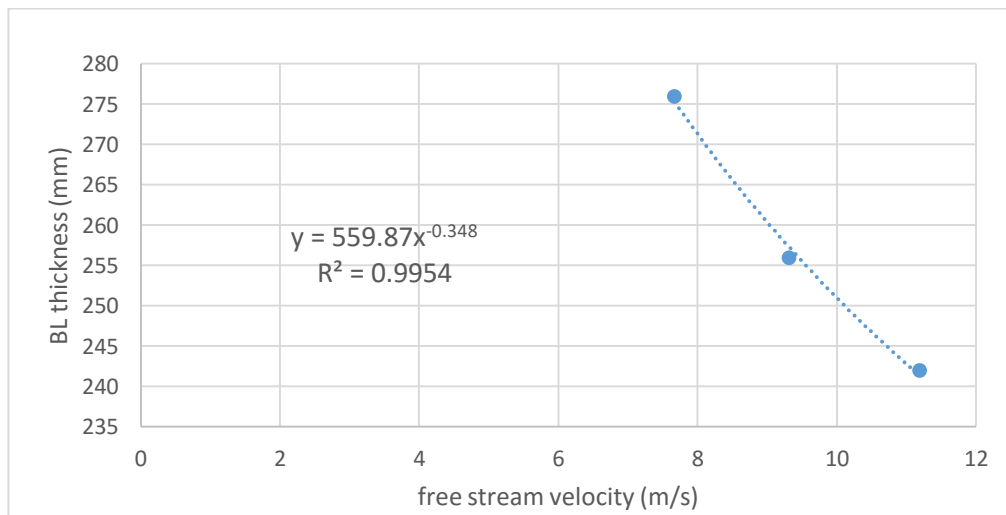


Figure 5.34: Velocity exponent determination for BL thickness

$$\delta = 559.87V^{-0.348}$$

$$b = -0.348$$

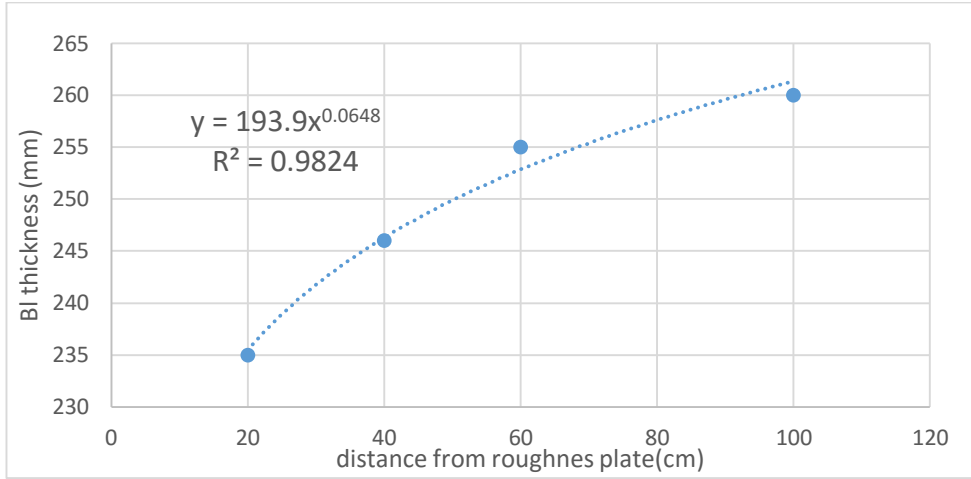


Figure 5.35: Distance exponent determination for BL thickness

$$\delta = 193.9X^{0.0648}$$

$$c = 0.0648$$

$$\delta = B[(z_0)^{0.5689}(V)^{-0.348}(X)^{0.0648}]^d$$

Now $(z_0)^{0.5689}(V)^{-0.348}(X)^{0.0648}$ consider as one system and vary only one independent variable but fixed other two variables, then correlate by using power equation

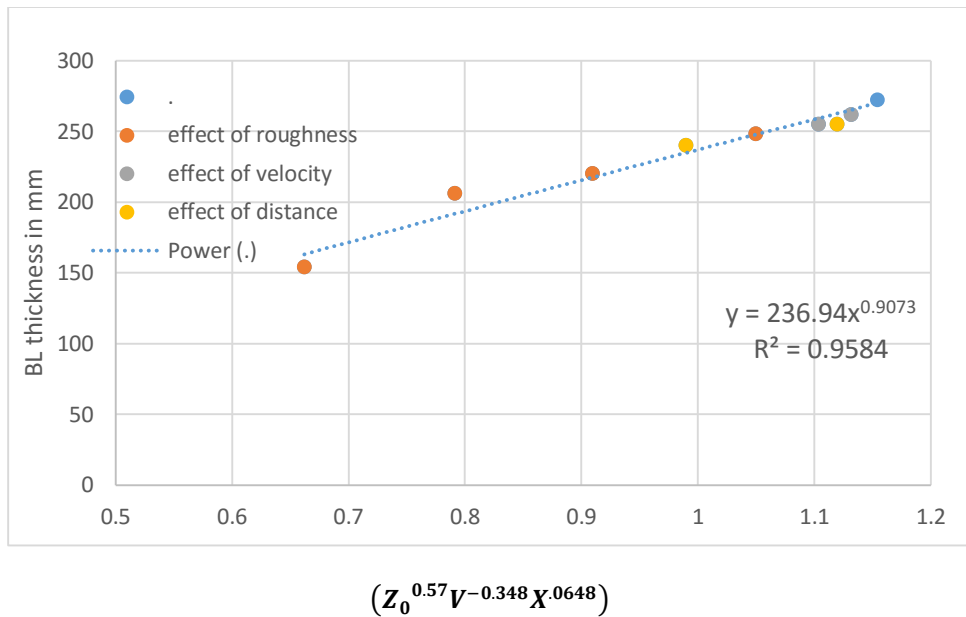


Figure 5.36: Correlation plot for system variable with BL thickness

$$y = 236.94x^{0.9073}$$

$$\delta = 236.94(Z_0^{0.57} V^{-0.348} X^{0.0648})^{0.9073}$$

5.8.2 Exponent's determination for displacement thickness:

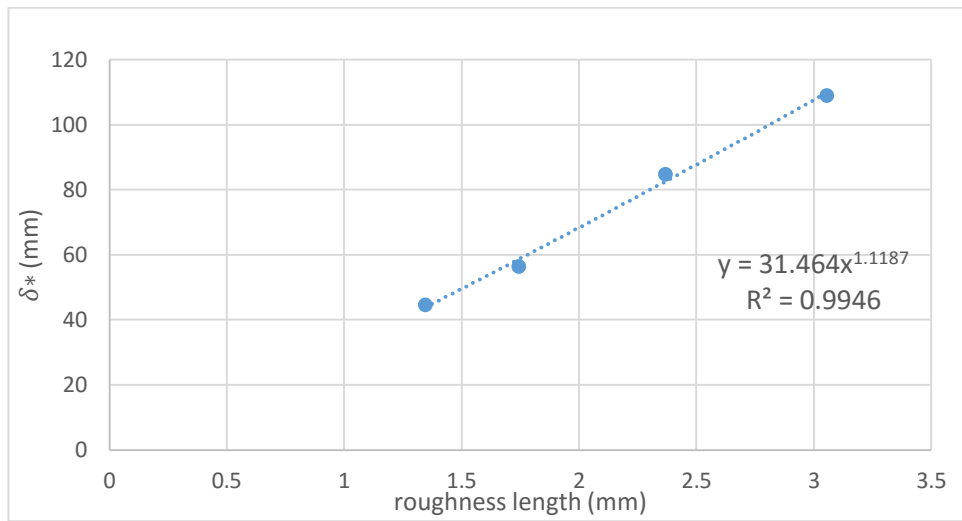


Figure 5.37: Roughness exponent for δ^*

$$\delta^* = 31.464Z_0^{1.1187}$$

$$a = 1.118$$

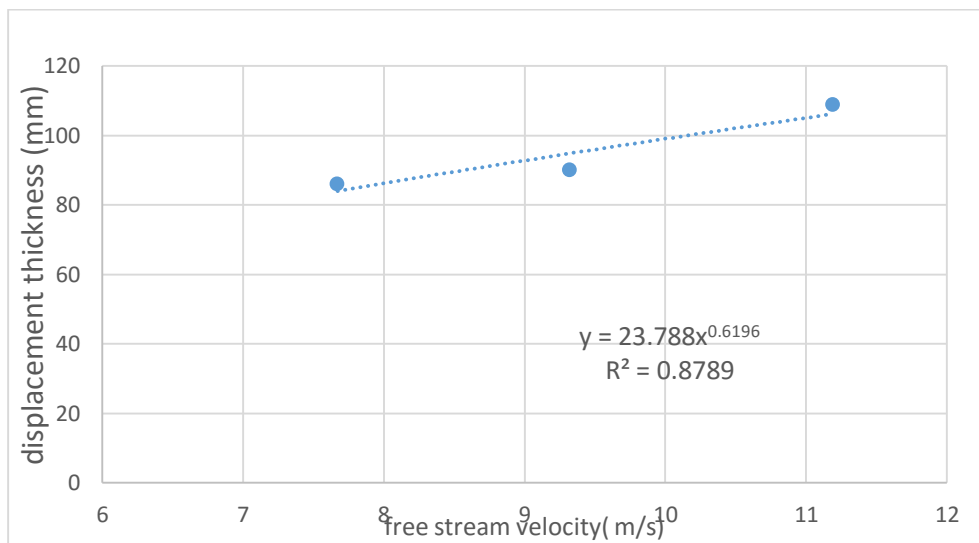


Figure 5.38: Estimation of Velocity exponent for δ^*

$$\delta^* = 31.464V^{0.6196}$$

$$b = 0.6196$$

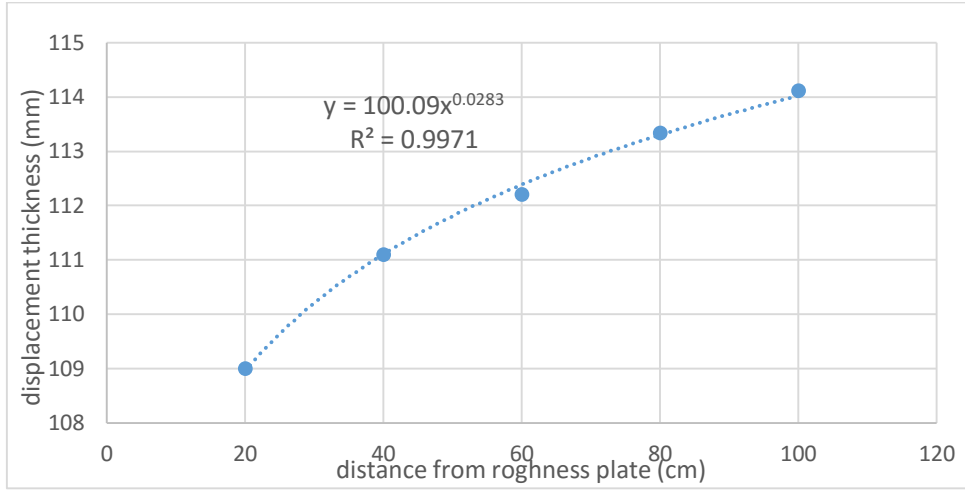


Figure 5.39: Estimation of exponent of X for δ^*

$$\delta^* = 100.09X^{0.0283}$$

$$c = 0.0283$$

$$\delta^* = B[z_0^{1.187}V^{0.619}X^{0.0283}]^d$$

Again correlate δ^* to whole function $(z_0^{1.187}V^{0.619}X^{0.0283})$ as one system

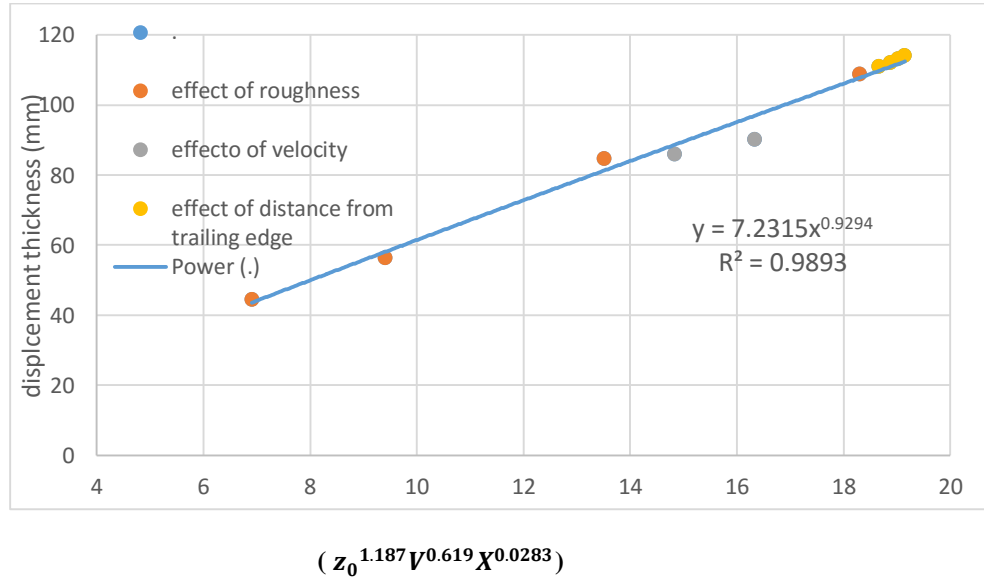


Figure 5.40: Correlation plot for system variable with δ^*

$$y = 7.2315x^{0.9294}$$

$$\delta^* = 7.2315(z_0^{1.187}V^{0.619}X^{0.0283})^{0.9294}$$

5.8.3 Correlation exponent's determination for Momentum thickness(θ):

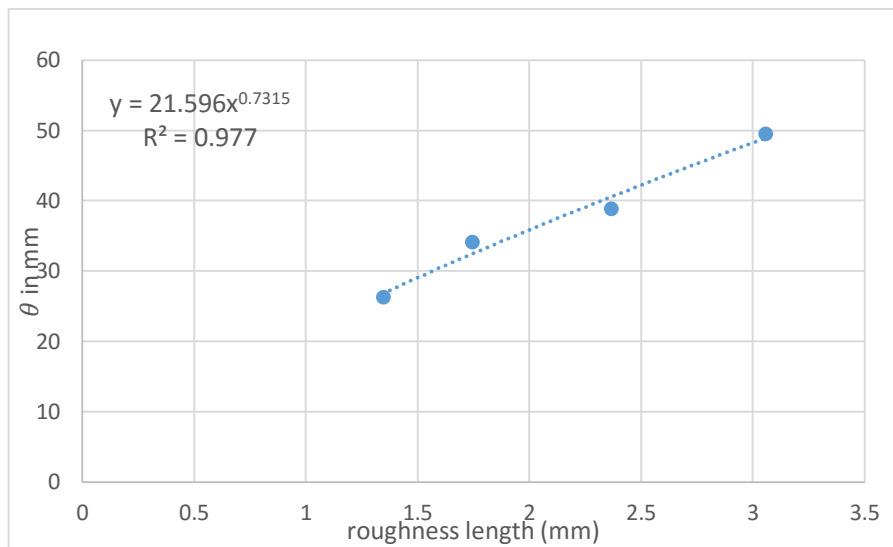


Figure 5.41: Estimation of roughness exponent for θ

$$\theta = 21.59Z_0^{0.7315} ,$$

$$a = 0.7315$$

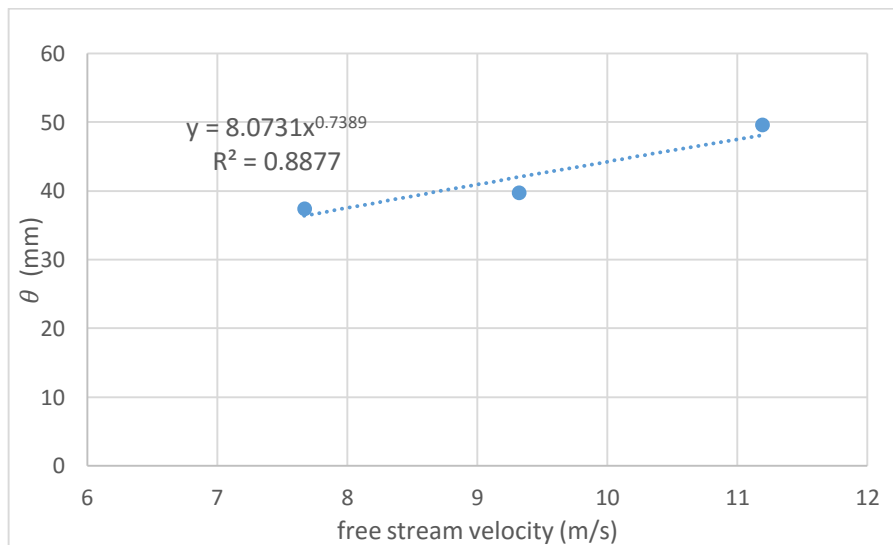


Figure 5.42: Estimation of velocity exponent for θ

$$\theta = 8.0731V^{0.7389}$$

$$b = 0.7389$$

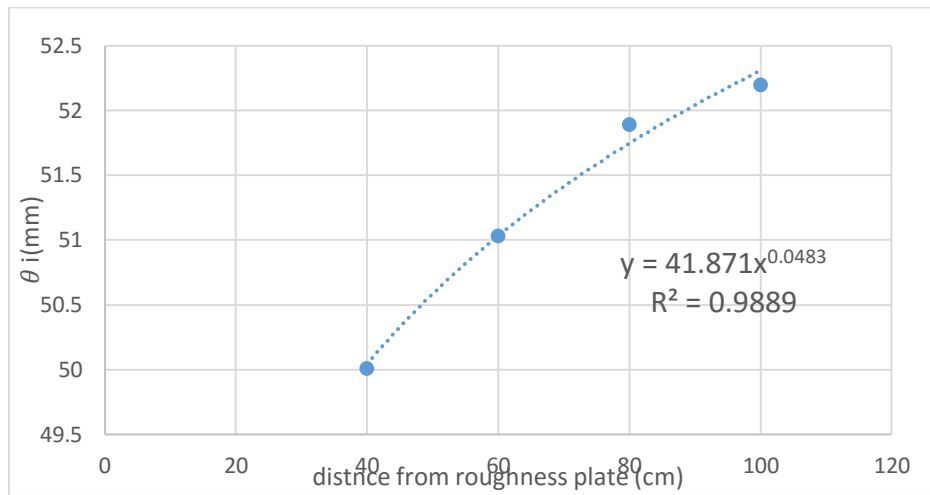
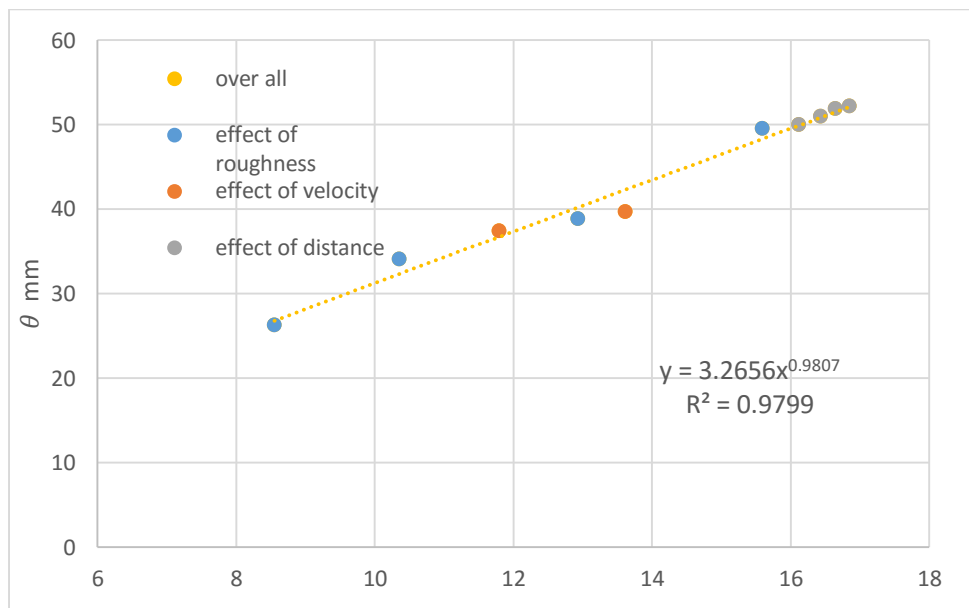


Figure 5.43: Estimation the exponent of X for θ

$$\theta = 41.871V^{0.0483}$$

$$c = 0.0483$$



$$(Z_0^{0.7315} V^{0.7389} X^{0.0483})$$

Figure 5.44: Correlation plot for system variables with θ

$$y = 3.2656x^{0.9807}$$

$$\theta = 3.265(Z_0^{0.7315} V^{0.7389} X^{0.0483})^{0.9807}$$

$$\delta, \delta^*, \theta = B[(z_0)^a(V)^b(X)^c]^d$$

Table 5.3: Values of exponents and constant for boundary layer parameters obtained from correlation

	a	b	c	d	Constant B
δ	0.57	-0.348	0.0648	0.9073	236.94
δ^*	1.187	0.619	0.0283	0.9294	7.23
θ	0.7315	0.7389	0.0483	0.9807	3.26

Table 5.4: Comparison between experimental and predicted value (δ) obtained from correlation

Roughness length(z) mm	Velocity in WT(m/s)	Distance from roughness plate (cm)	Experimental value of(δ) mm	Predicted value (δ) mm	Error (%)
3.056	11.19	20	235	234.94	-0.03
2.367	11.19	20	194	205.82	6.09
1.745	11.19	20	176	175.80	-0.10
1.345	11.19	20	138	148.00	-6.75
3.056	11.19	40	224	234.66	4.75
3.056	11.19	60	231	240.56	4.14
3.056	11.19	80	242	250.82	3.64
3.056	11.19	100	252	258.20	2.46
3.056	7.67	20	238	244.64	2.70
3.056	9.32	20	230	238.85	3.80
3.056	11.19	20	223	234.94	5.35

Table 5.5: Comparison between experimental and predicted value of (δ^*) obtained from correlation

Roughness length(z) mm	Velocity in WT(m/s)	Distance from trailing edge (cm)	Experimental value of(δ^*) mm	Predicted value (δ^*) mm	Error (%)
3.056	11.19	20	109.00	107.66	1.20
2.367	11.19	20	84.83	81.21	4.40
1.745	11.19	20	56.46	58.02	2.70
1.345	11.19	20	44.61	43.53	2.07
3.056	11.19	40	111.10	109.64	1.31
3.056	11.19	60	112.20	110.85	-1.20
3.056	11.19	80	113.34	111.65	-1.40
3.056	11.19	100	114.12	112.32	-1.54
3.056	7.67	20	86.12	86.63	0.59
3.056	9.32	20	90.22	96.91	7.43
3.056	11.19	20	109.00	107.66	1.21

Table 5.6: Comparison between experimental and predicted value of (θ) obtained from correlation

Roughness length(z) mm	Velocity in WT(m/s)	Distance from trailing edge (cm)	Experimental value of(θ) mm	Predicted value (θ) mm	Error (%)
3.056	11.19	20	49.53	48.25	-2.58
2.367	11.19	20	38.90	40.17	3.20
1.745	11.19	20	34.11	32.28	-5.36
1.345	11.19	20	26.27	26.78	1.9
3.056	11.19	40	50.01	49.86	-0.4
3.056	11.19	60	51.03	50.83	-0.04
3.056	11.19	80	51.89	51.53	-0.10
3.056	11.19	100	52.20	52.08	-0.23
3.056	7.67	20	37.40	36.70	-1.80
3.056	9.32	20	39.67	42.26	6.57
3.056	11.19	20	49.53	48.25	-2.58

5.9 COMPARISON GRAPHS FOR BOUNDARY LAYER PARAMETERS:

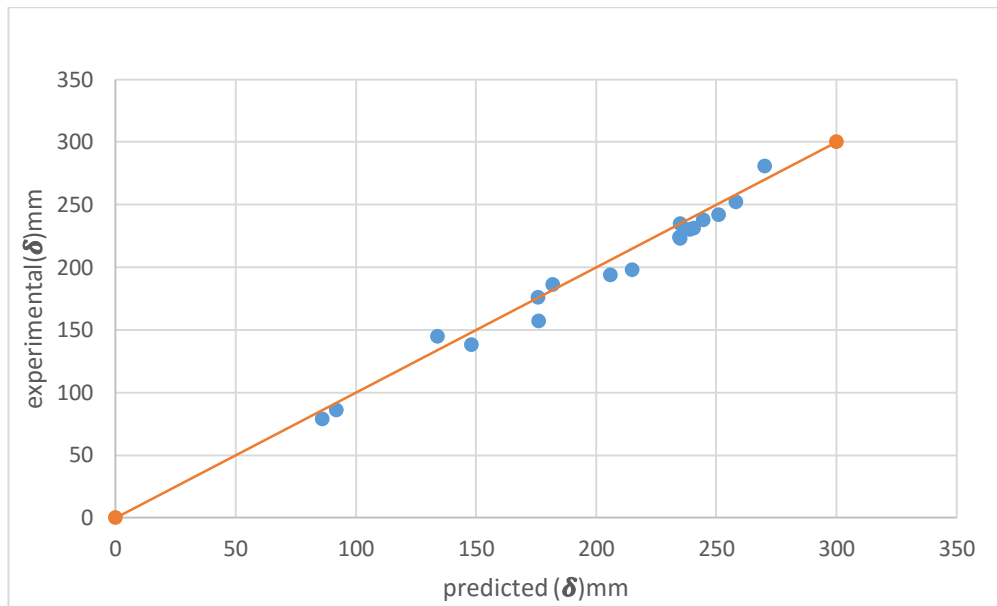


Figure 5.45: Comparison between experimental and predicted (δ)

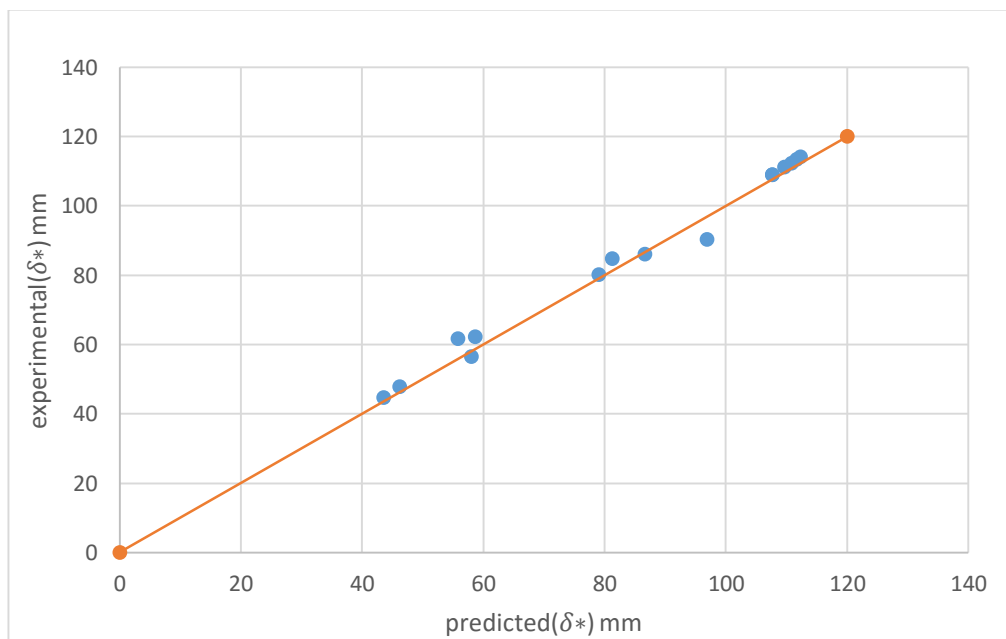


Figure 5.46: Comparison between experimental (δ^*) and predicted (δ^*)

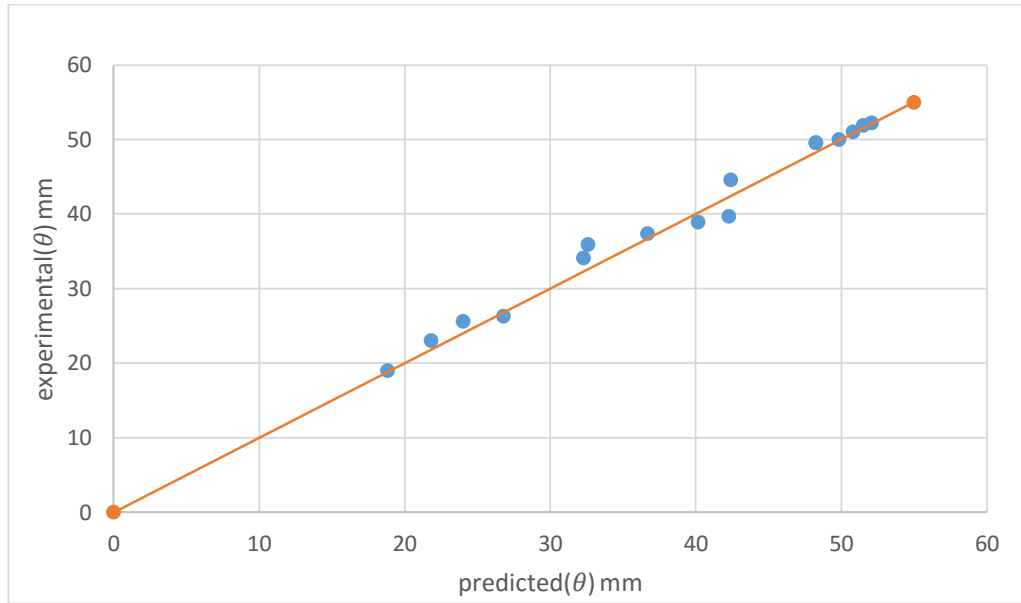


Figure 5.47: Comparison between experimental (θ) and predicted (θ)

5.10 DISCUSSION

Results are shown in above graphs and tables. In Fig no.5.1 to fig no.5.6 the velocity profiles explains the effect of different arrangements of spires and blocks on boundary layer in test section of Wind Tunnel. It has been found that diamond arrangement are more effective in producing higher BL depth compare to that of square arrangement and BL depth increases with increase in longitudinal distance from the last point roughness plate. Combination of spires with diamond pattern of block increases maximum BL thickness compare to other arrangements of spires and blocks, it has been found that spire with blocks are more effective in producing higher BL depth compare to that of only blocks because in blocks pattern, main reason is momentum deficit and turbulence is higher due to wake formations in wind tunnel. In fig no.5.18 to 5.21 using log- law, explain that roughness thickness is maximum for spires with diamond pattern of blocks so turbulence is higher and it increases more BL thickness. At constant main stream velocity boundary layer depth increases as roughness thickness of the patterns increase. One thing is important that spires were more effective to produce a thicker BL compare to that produced by different blocks arrangements, for blocks arrangement BL thickness increases due to momentum deficit but for spires arrangement wake formations. For a particular roughness pattern and constant main stream velocity BL thickness increases as longitudinal distance increases form the roughness plate. If velocity increases for a particular pattern than BL depth decreases.. The values of boundary layer parameters are calculated by putting the equations obtained from graphs γ/δ vs. v/V in the theoretical formulas are shown in

fig.no.5.22 to fig.no 5.32 and all obtained values of BL parameter tabulated in Table.no 5.2 Further these values used for establishment of correlation between dependent variables and system variables. Exponents of system variables are estimated by using power equations for BL parameters are shown in shown in fig no.5.35 to fig.no.5.44 and exponents and constant values obtained from correlation are tabulated. Comparison graphs are plotted between experimental values of BL parameters and predicted values obtained from correlation

CHAPTER 6: CONCLUSIONS

6.1 CONCLUSIONS

From this experimental work and data analysis, conclusions have been made which are given below-

1. In test section of plane surface empty Wind Tunnel maximum boundary layer depth is 9cm to 11 cm.
2. BL thickness increase with decrease in main stream velocity.
3. The boundary layer depth increases in test section as the longitudinal distance from the roughness plate increases.
4. The square arrangement and diamond arrangement with 5 cm spacing of 1 inch blocks, is effective in producing a BL depth up to a maximum of 1.4 and 1.8 times in the test section as compared to that of the plane surface wind tunnel.
5. Using the experimental data and log-law, roughness thickness is estimated for all configuration. Roughness thickness has been found to increase in this particular order: square pattern, diamond pattern of blocks, spires with square pattern of blocks and spire with diamond arrangement.
6. BL thickness increases with increase in roughness for a constant velocity.
7. Spires's arrangement increases the boundary layer depth with decrease in spacing between them for a constant velocity. It has been found that, for a 6cm c/c spacing of spires, the produced BL depth ranges between 190 % and 220% as compared to plane surface WT
8. Combination of spires with different pattern of blocks are effective in producing BL thickness which ranges between 250% to 300% of empty wind tunnel and it is more effective in producing a thicker boundary layer than that produced by using only spires or different arrangement of blocks produced in test section.
9. The B/L thickness, displacement thickness and momentum thickness increase with increase in roughness parameter. While for increase of mainstream velocity all the parameters increase except B/L thickness

6.2 SCOPE FOR FUTURE WORK

Actually most Wind Tunnel is designed which having boundary layer depth is very less and turbulence intensity is not more than 0.5% so by using of different arrangements of blocks and spires we can enhance the boundary layer and turbulence intensity. Atmospheric boundary layer thickness vary from 1km to 2 km on earth surface and every civil structures are within ABL. Testing model should be with in boundary layer in test section of wind tunnel to get real effect of fluid flow on model. Turbulence intensity is important property of wind it depends on characteristics of ground whereas in test section of wind tunnel is plane. We can simulate the atmospheric boundary layer in wind tunnel by using different arrangement passive device according to the terrain characteristics. The scope for this project relies on the theory that boundary layer exists everywhere in this world so considering turbulence, an essential part one can determine the parameters within permissible limits for safe design of structures or any construction and many other fields like industries.

1.REFERENCES

2. Irwin, H.P., "The design of spires and strips for wind simulation," *journal of wind Engineering and industrial Aerodynamics* 7:361-366(1981)
3. Cermak, J.E., "Physical modeling of the Atmospheric boundary layer in short boundary layer wind tunnel," (1982)
4. Dumitrescu ,I.S., "Roughness elements geometry required for wind tunnel Simulation of the atmospheric wind,"-Transactions of the ASME, New York, Journal of fluids Engineering 99:480-485(1977)
5. Cook, N.J. "Wind-Tunnel Simulation of the Adiabatic Atmospheric Boundary Layer by Roughness, Barrier and Mixing Device Methods." *Journal of Industrial Aerodynamics* 3 (1978): 157-176.
6. Counihan, J. "An Improved Method of Simulating an Atmospheric Boundary Layer in a WIND TUNNEL Atmospheric Environment 3 (1969): 197-214
7. Farell, Cesar, and Iyengar, Arun K.S. "Experiments on the Wind Tunnel Simulation of Atmospheric Boundary Layers." *Journal of Wind Engineering and Industrial Aerodynamics* 79 (1999): 11-35.7- Stevenson T. "Report on the simultaneous observations of the force of the wind at different heights above the ground." *J Scot. Met. Soc.* 5, 348-351,1880
9. Suniu, E. and Scanlan, R. *Wind Effects on Structures (3rd edition)*. John Wiley & Sons, Inc., New York, N.Y., 1996
10. C.F. Cowdrey, A simple method for the design of wind tunnel velocity profile grids, Natl. Phys. Lab. (U.K.), Aero Note 1055 (May 1967).
11. G.S. Campbell and N.M. Standen, *Simulation of earth's surface winds by artificially thickened wind tunnel boundary layers, Progress Report* , National Research Council of Canada, NAE Rep. LTR-LA-37 (July 1969).
12. Garratt, J.R. *The Atmospheric Boundary Layer*, Cambridge University Press, New York, NY, 1992
13. Sutton O. G. *Atmospheric Turbulence*. Methuen, London, 1949.
14. Chapman, R. K. and Gouveia, F. J., *Building III Wind Flow Study: July 1987*, Lawrence Livermore National Laboratory, Livermore, California, 1987.
15. A.G. Robins, *The development and structure of simulated neutrally stable atmospheric Boundary layers*, J. Ind. Aerodyn. 4 (1979) 71-100.

16. Castro, I.P., Robbins, A.G., “The Flow Around a Surface-Mounted Cube in Uniform and Turbulent Streams,” *Journal of Fluid Mechanics* 79(2):307–335 (1977).
17. Gomes, M.G., Moret Rodrigues, A., and Mendes, P., “*Experimental and Numerical Study of Wind Pressures on Irregular-Plan Shapes*,” *Journal of Wind Engineering and Industrial Aerodynamics* 93(10):741–756 (2005)
18. Stathopoulos, T., “*Design and Fabrication of a Wind Tunnel for Building Aerodynamics*,” *Journal of Wind Engineering and Industrial Aerodynamics* 16:361–376 (1984).
19. Stathopoulos, T., and Dumitrescu-Brulotte, M., “*Design Recommendations for Wind Loading on Buildings of Intermediate Height*,” *Canadian Journal of Civil Engineering* 16(6):910–916 (1989)
20. R.I. Harris, *Longer turbulence length scales*, *J. Wind Eng. Ind. Aerodyn.* 24 (1986) 61-68.
21. H.W. Tieleman, Problems Associated with flow modeling procedures for low-Rise structures, *J. Wind Eng. Ind. Aerodyn.* 42 (1992) 923-934
22. J. Yee-Tak Ng, *The structure of the turbulent flow at the test section of BLWT II*, E.S. 400 Project Report, Faculty of Engineering Science, University of Western Ontario, 1986.
23. J. Counihan, *Wind tunnel determination of the roughness length as a function of the fetch and the roughness density of three-dimensional roughness elements*, *Atmos. Environ.* 5 (1971) 637-642.
24. D.E. Coles, *The law of the wake in the turbulent boundary layers*, *J. Fluid Mech.* 1 (1956) 191-226.